Mechanochemical Principles of Spatial and Temporal Patterns in Cells and Tissues

Anaïs Bailles, Emily Gehrels, Thomas Lecuit

Mechanochemical principles of spatial and temporal patterns in cells and tissues

Anaïs Bailles,[1#] Emily W. Gehrels,[2#] and Thomas Lecuit[2,3,*]

[1] Max Planck Institute of Molecular Cell Biology and Genetics, Pfotenhauerstraße 108, 01307 Dresden, Germany
[2] Aix Marseille Université & CNRS, IBDM - UMR7288 & Turing Centre for Living Systems, Campus de Luminy Case 907, 13288, Marseille, France
[3] Collège de France, 11 Place Marcelin Berthelot, Paris, France

* Corresponding author, email: thomas.lecuit@univ-amu.fr
# These authors contributed equally to this article

Shortened running title:
Mechanochemical patterns in biology

Keywords: patterns, morphogenesis, Turing, oscillations, excitability, mechanochemical processes

Abstract

Patterns are ubiquitous in living systems and underlie the dynamic organization of cells, tissues and embryos. Mathematical frameworks have been devised to account for the self-organization of biological patterns, most famously the Turing framework. Patterns can be defined in space, for example to form stripes, in time such as during oscillations, or both to form traveling waves. The formation of these patterns can have different origins: purely chemical, purely mechanical, or a combination of the two. Beyond the variety of molecular implementations of such patterns, we emphasize the unitary principles associated with them, across scales, in space and time, within a general mechano-chemical framework. We illustrate where such mechanisms of pattern formation arise in biological systems from the cellular to tissue scales with an emphasis on morphogenesis. We wish to convey a picture of pattern formation that draws attention to the principles rather than solely specific molecular mechanisms.

1. INTRODUCTION

A pattern is a repeated feature in the organization of the components of a system, whether molecules in a cell, cells in a tissue, or organisms in an ecosystem. Pattern formation is a key step in the development of all organisms as it leads to the emergence of structures, which later support function. For instance, villi in the gut increase the surface area of exchange between the bloodstream and the intestinal lumen (Walton et al. 2018), and the non-random distribution of feather buds sets up the spatial distribution of feathers in the young bird (Shyer et al. 2017). At the cellular scale, patterns can be associated with cell polarization, such as in motile

eukaryotic cells (Houk et al. 2012), or cell differentiation, such as actin-rich microvilli (Delacour et al. 2016) and microridges (Depasquale 2018), or microtubule rich stereocilia (Wagner & Shin 2019) in epithelial cells.

A pattern can be observed as a regular (non-random) variation in molecule concentration or alignment in a cell, in cell types or states in a tissue, or in positions, densities, and orientations of components either in a tissue or among organisms. Patterns may also occur in time: an activity may emerge and subsequently persist, vanish or oscillate. The regularity of the variation has a characteristic period in space or time. The period of the pattern can be orders of magnitude larger than the components involved: molecules with a size of a few nanometers can produce patterns on the order of microns; cells with a size of a few microns can give rise to patterns on the order of a few hundreds of microns; molecular binding times of less than a second can produce oscillations more than one hundred times longer. How can patterns form at much larger scales than their components?

Patterns are said to be self-organized when they emerge from homogeneous, isotropic systems. In principle, this means there is no pre-pattern. However, in biological systems some pre-pattern often coexists with some degree of self-organization (Collinet & Lecuit 2021). At the cell scale, pre-patterning can take the form of cellular components that are non-uniformly distributed to begin with, as is often the case in newly laid eggs. For example, pattern formation in the *Drosophila* embryo requires an inherent broken symmetry in the egg based on the position of maternally-deposited RNA (Roth & Lynch 2009). At the tissue scale, pre-patterned localization of molecules along certain directions (e.g. on vertical versus horizontal cell junctions) can lead to cell intercalation and tissue flow in many systems (Lecuit et al. 2011). In this review, we focus on how patterns can theoretically arise from interactions among

components of a system independently of any external cue. The experimental examples we present rely mainly on self-organization, but some degree of pre-pattern is often present.

Generally speaking, interactions between components of a system allow patterns to form spontaneously through growth and stabilization of a fluctuation, as described in Section 2.1. The stabilized fluctuations can be spatial (Sections 2.1, 2.2, 3.1, 3.2), temporal (Sections 2.3, 3.3), or both (Sections 2.4, 3.4). This principle holds regardless of the nature of the interaction: it can be purely chemical as initially investigated by Turing (Section 2), but can also be mechanical, or even mechanochemical (Section 3), and can occur at different length scales.

2. SPONTANEOUS FORMATION OF CHEMICAL PATTERNS

2.1. The theory of Turing patterns

There exist several theoretical models for how spatial patterns can spontaneously form in an initially uniform medium (Gierer & Meinhardt 1972; Rashevsky 1940; Segel & Jackson 1972; Turing 1952). Here we will work through the basic logic arising from a selection of these models to build a basic understanding of their defining features. Detailed discussion of this type of model can be found in several other reviews (Halatek et al. 2018; Hiscock & Megason 2015; Howard et al. 2011; Koch & Meinhardt 1994; Kondo & Miura 2010; Schweisguth & Corson 2019; Wedlich-Söldner & Betz 2018).

We begin by considering models where the medium is composed of diffusive species that interact chemically. The interactions are assumed to be such that the system is initially in stable equilibrium, but that a variation of the parameters can cause the equilibrium to become unstable (Segel & Jackson 1972; Turing 1952). Exposure of an unstable system to perturbations, such as thermal fluctuations, will cause it to depart from equilibrium, allowing non-uniformities in

the concentrations of the constituent species to develop. Under certain conditions, some wavelengths of concentration variations will be selectively amplified from the initial fluctuations, thus creating patterns (Figure 1A). These patterns are often referred to as Turing patterns as they were most famously described by Turing in 1952.

Turing's pioneering contribution was his mathematical treatment of interacting and diffusing species using a system of reaction-diffusion equations:

$$\partial C_i/\partial t = D_i \nabla^2 C_i + R_i(C_1, C_2, \ldots, C_n) \quad (1)$$

where the subscripts, $i = 1 \ldots n$, refer to the n different species, C_i are their concentrations, D_i are their diffusion constants, R_i are the cross-reactions between the species, and $\nabla^2 \equiv \partial^2/\partial x^2 + \partial^2/\partial y^2$. These equations describe the changes in concentration of each species in the solution as a function of their diffusion constants and their cross-reactions with one another. To simplify these equations, Turing considered the simple case of only two species interacting. He also worked under the assumption that the concentrations did not vary greatly from their original uniform distribution, and so all terms non-linear in these variations could be neglected. These considerations allowed him to provide a mathematical description that was solvable analytically under certain conditions.

In his article, Turing explored the general solutions of reaction-diffusion equations in different physical scenarios. He found that the solutions took the form of sums of terms, each containing a sinusoidal spatial component multiplied by a component that grows or shrinks exponentially in time. All terms in this sum are negligible compared with those that grow the fastest. His main finding was that, under certain conditions, it is possible for the solutions to yield a stationary wave pattern. He gave examples of reactions that would yield this behavior, and

some general mathematical conditions, but did not provide an intuitive interpretation of these conditions.

Segel and Johnson's 1972 article described in depth the conditions for the appearance of spatial patterns with finite wavelength in a two-species system. To achieve the stationary wave case discovered by Turing, they found that it was necessary for one species to act as an inhibitor that decreases the concentration of both species and for the other to act as an activator that increases the concentration of both species. They also showed that it was necessary for the inhibitor to diffuse faster than the activator (Figure 1B left).

In 1972, Gierer and Meinhardt independently proposed the need for an activator and an inhibitor with diffusion of the inhibitor greater than that of the activator. They also proposed that the depletion of a substance that is consumed during activation can play the role of a long-range inhibition (Figure 1B right). While they drew some similar conclusions to earlier works, their model also included non-linear interaction terms. The inclusion of nonlinear terms (see also (FitzHugh 1961; Gray & Scott 1984; Thomas 1976)) was an important development since the types of patterns formed by reaction-diffusion equations depend strongly on their nonlinearity (Barrio et al. 1999; Ermentrout 1991; Maini 2004; Oster & Murray 1989). Some examples of patterns that can be produced by these models are shown in Figure 1C.

There has been much debate about what constitutes a Turing pattern and whether or not these simple models can be relevant in inherently complex biological systems. We chose to refer broadly to ‘Turing-like’ patterns, where the diffusion of chemicals can be replaced by spatial coupling caused by more complex chemical or cellular phenomena (Hiscock & Megason 2015). In the sections that follow, we introduce examples where these models accurately

predict biological behavior, first in the formation of static patterns as discussed above, then for the more complex cases of temporal oscillations and waves.

2.2. Turing patterns in biological systems

While the models described above are grossly simplified, they can provide insight into real biological systems. The simplest pattern is a variation in the concentration of one species along a single axis, known as polarity. Polarization is a key stage in the morphogenesis of many species, and is often triggered by the prepatterning of small molecules such as GTPases (Park & Bi 2007). However, there exist cases where polarity can occur spontaneously in the absence of pre-existing spatial cues.

This is true for budding yeast (*Saccharomyces cerevisiae*) (Figure 1D), which, when mutated to remove spatial landmarks, still polarize to form a single bud at a random location (Bender & Pringle 1989; Chant & Herskowitz 1991; Howell et al. 2012). The location of the bud is determined by the spontaneous formation of a gradient of the GTPase Cdc42 (Halatek et al. 2018; Park & Bi 2007). Several models have been developed that demonstrate that this polarization can arise through a Turing mechanism (Borgqvist et al. 2021; Goryachev & Pokhilko 2008; Howell et al. 2012). The role of the activator is played by the active, membrane-bound form of Cdc42, which can autocatalytically recruit more active Cdc42. The inhibition is caused by the substrate depletion of the inactive, cytosolic form of Cdc42, as it is effectively consumed to form active Cdc42 (Figure 1D). The validity of these models has been supported by different experimental perturbations, where components of the system are removed or constitutively activated (Howell et al. 2012; Irazoqui et al. 2003; Wedlich-Soldner et al. 2003). Spontaneous polarization on the cellular scale also exists in other systems, such as during cell motility in *Dictyostelium discoideum* (Iglesias & Devreotes 2008).

Turing patterns in biological systems are not limited to simple polarity and single cells. At the subcellular level, molecules can form patterns of spots at the scale of hundreds of nanometers (Kryuchkov et al. 2020). At the tissue level, interactions between cells can also lead to Turing patterns. One biological example of a tissue level pattern is the formation of rugae that form the mouse palate (Economou et al. 2012). Rugae formation aligns with a striped pattern of *Shh* expression, which occurs as a result of the interaction between FGF signaling that acts as an activator and Shh signaling that acts as an inhibitor (Figure 1E). Other examples include: body axis determination (Müller et al. 2012; Rogers et al. 2017; Sekine et al. 2018), and branched or stripped organ patterns (Menshykau et al. 2019; Scoones & Hiscock 2020).

Another example of a striped pattern is the regular pattern of digits in vertebrates, which can be modeled using a three-node network composed of Sox9, Wnt, and Bmp (Newman & Frisch 1979; Raspopovic et al. 2014). This generates a Turing instability based on three components instead of the classical activator-inhibitor pair. Though in this review we focus mainly on systems that follow the typical two-component model, there exist many possible network topologies with two or more components that can lead to pattern formation (Scholes et al. 2019). The vast majority of Turing pattern generating networks contain two core motifs: a positive feedback on one of the diffusing components, and a negative feedback on another more rapidly diffusing component (Scholes et al. 2019).

The ingredients of Turing pattern formation can even hold between individuals. For example, it has been shown that ants cluster their dead into piles following a Turing mechanism (Theraulaz et al. 2002). Local activation arises because the probability of a worker ant depositing a dead individual in an existing pile grows with the size of the pile, and inhibition

arises from a depletion of dead in the surroundings (Figure 1F). Large-scale Turing pattern formation also exists in the patterns in expanding populations of genetically programmed *E. Coli* cells (Liu et al. 2011), and could also play a role in the formation of the intricate structure of insect nests (Heyde et al. 2021; Khuong et al. 2016; Perna & Theraulaz 2017).

There are also cases where it is not clear whether or not a pattern arises from a Turing mechanism. For example, early investigations into stripe formation in fish found that interactions between different types of pigment cells followed a local activation, long-range inhibition mechanism and concluded that the stripes were Turing patterns (Frohnhöfer et al. 2013; Nakamasu et al. 2009). However, it was later shown that the interactions between the pigment cells were regulated by cell projections instead of diffusion (Eom et al. 2015; Mahalwar et al. 2014) and that therefore, while the criteria for local activation and long-range inhibition still held, it did not fit the traditional reaction-diffusion requirements of a true Turing pattern (Watanabe & Kondo 2015a,b). Even more recently, it has been suggested that growth of the tissue is important for stripe formation as well (Owen et al. 2021). This pattern could thus be said to be formed by a 'Turing-like' mechanism, where cell motion takes the role of molecular diffusion in the original Turing mathematical model.

Overall, these examples demonstrate the breadth of biological systems that rely on Turing or Turing-like mechanisms for pattern formation. It appears that the general requirements of local activation and long-range inhibition (or substrate depletion) can lead to the appearance of patterns across a wide range of interaction types and scales.

2.3. Temporal oscillations

We now focus on how temporal oscillations arise. There is a strong analogy between spatial and temporal pattern formation. In the former case, a standing wave can be produced by an activator and an inhibitor, with different diffusion coefficients. In the latter case, a temporal wave can be produced by an activator and an inhibitor, with a time delay in the inhibition (Figure 2A). We mainly describe activator-inhibitor systems, but other networks can give rise to oscillations based on more complex feedback loops. The general ingredients for oscillations in chemical systems are delayed negative feedback and non-linearity (Beta & Kruse 2017; Novák & Tyson 2008). A time delay can come from intermediate chemical reaction steps involving more chemical species. The dynamics of two-component systems can be visualized using a phase plot, which shows the concentration of one species on each axis; a point on the graph represents the two concentrations at a given time point. Given the ingredients mentioned above, and careful parameter choices, a limit cycle (or a closed loop) can appear in the phase plot, revealing the existence of oscillations (Figure 2A right).

A historical example of an oscillatory system is the predator-prey model described by Lotka (Lotka 1920) and Volterra (Volterra 1926). The population of predators grows when a predator catches a prey, hence proportionally to the population of the prey times that of the predators (a non-linear effect). An increase of prey thus progressively causes a progressive increase of predators. Conversely, the predators slowly consume the prey population according to a similar non-linear equation, decreasing the prey population after a delay. When the prey population becomes too small, the predator population declines, allowing the prey population to expand again. As a result, each population oscillates with the same period but with a phase difference (Figure 2A). Intuitively, the time delay here results from the time needed for the predator population to grow before it starts decreasing the prey population.

Many examples of oscillating systems exist in biology, involving glycolysis (Pye & Chance 1966), cAMP (Gerisch et al. 1975), the cell cycle and cyclins (Evans et al. 1983), and somite clock genes (Palmeirim et al. 1997). One function of these oscillations is to implement a biological clock. The most famous example is probably the animal circadian clock (Bargiello & Young 1984; Bargiello et al. 1984; Konopka & Benzer 1971; Reddy et al. 1984; Zehring et al. 1984). Oscillating reaction network can convey information through both amplitude (molecule concentration) and frequency encoding (Cai et al. 2008; Li et al. 1998; Purvis & Lahav 2013; Yang & Wu 2018).

An important subset of oscillatory systems is oscillatory excitable systems (Ferrell et al. 2011; Gelens et al. 2014). In addition to delayed inhibition, oscillatory excitable systems include a strong positive feedback loop of the activator onto itself, as in the example of the FitzHugh-Nagumo model (Ferrell et al. 2011) (Figure 2B). Above a threshold, there is an abrupt increase in activator concentration (Figure 2B). After a delay, the inhibitor causes an abrupt decrease of the activator concentration back to the initial value, completing one cycle of relaxation oscillations. In a phase plot, a slow increase/decrease in concentration approximately follows the activator nullcline (the line where the partial time derivative of the activator is zero), while a fast increase/decrease happens when the system jumps from one point on the nullcline to the next, as in a hysteretic switch (Figure 2B). The added positive feedback allows for a wider range of frequencies without changing the amplitude, and also allows oscillations to occur over a wider range of parameters (Tsai et al. 2008), thereby enhancing the system robustness (Beta & Kruse 2017). In many biological cases, a refractory period follows the de-excitation: no stimulus is able to trigger the excitation again for some finite time, which corresponds for example to the degradation time of the inhibitor. Most biological oscillatory systems are oscillatory excitable systems.

An example of an oscillating excitable system is *Dictyostelium* cell migration, which is controlled by two oscillatory systems with different time scales (Figure 2C,D,E) (Huang et al. 2013). The fast-oscillating system (CON) is based on actin and its regulatory proteins SCAR/WAVE, Arp2/3 and a negative feedback mediated by Coronin. It results in small undulations of the cell edge, but is ready to be excited, like an idling motor. The slow-oscillating system (STEN) is based on a positive feedback involving Ras, PI(3)K and Rac, and also displays waves. The STEN and CON oscillators are coupled via Rac. Thereby, the slow-oscillating system can stimulate the fast-oscillating one (Figure 2E, left) to produce larger stable cell protrusions (Figure 2E, right) which promotes cell migration (Huang et al. 2013). The slow oscillating system is excitable, as shown by the presence of a refractory phase and a maximal response to any stimuli above a threshold (Huang et al. 2013).

Oscillations can be synchronized in space, either through a pacemaker or through local interactions, resulting in collective oscillations. Circadian clocks are entrained by environmental cues, such as light (Ceriani et al. 1999; Emery et al. 1998). In mammals, the hypothalamus entrains the peripheral clocks via hormones (reviewed in (Buijs & Kalsbeek 2001)). Collective oscillations also exist within groups of organisms. For example, fireflies can flash collectively (Morse 1916). At high enough density, the firefly flashes (around 2 per second) are synchronized with millisecond precision by visual feedback between individuals (Buck & Buck 1968; Sarfati et al. 2021). Interestingly, some wave patterns have also been observed in firefly swarms (Sarfati et al. 2021).

2.4. Spatiotemporal patterns

Chemical networks can also generate traveling waves when spatial coupling acts on top of oscillatory, bistable, or excitable dynamics (Gelens et al. 2014). Waves based on spatial coupling, hence physical in nature, are different from kinematic or pseudo- waves, which result from a pre-established phase shift between oscillators. Physical waves can be identified because the wave can be stopped using a physical isolation or barrier. In contrast, kinematic waves are not stopped by barriers.

The spatial coupling needed to form physical waves can be provided by diffusion in an excitable or a bistable system. A small increase in the activator concentration above a threshold is amplified by a positive feedback loop, bringing the excitable or bistable system to a state with high activator concentration. Now, if the activator is allowed to diffuse, it will cause the neighboring concentration to exceed the threshold, thus getting pushed to high concentration (Figure 3A). Hence, a wave of activation will propagate spatially in the medium, as a trigger wave. This requires the diffusion to be slow compared to the characteristic time of the positive feedback loop (Gelens et al. 2014). This prevents diffusion from decreasing the concentration too much before the feedback has time to act (Figure 3A). A single mathematical model of excitable systems, such as the FitzHugh-Nagumo model (FitzHugh 1961), can exhibit spatial, temporal, and spatiotemporal patterns (waves) depending on the parameters (Gelens et al. 2014).

Traveling waves can occur in cell-scale systems, where diffusion provides spatial coupling (reviewed in (Beta & Kruse 2017; Yang & Wu 2018)). In the bacteria *Escherichia coli*, the division regulator proteins MinC, MinD and MinE oscillate at the poles of the rod-like bacteria (de Boer et al. 1989; Hu & Lutkenhaus 1999; Raskin & Boer 1999; Wettmann & Kruse 2018) and define a zone of lower activity in the center where the fission apparatus is assembled. Min

proteins can also form waves *in vitro*, which can be modeled by cooperative binding of proteins at the membrane and diffusion, with non-linearity (Loose et al. 2008). *In vivo*, usually only oscillations are present, but traveling waves can appear in the case of a growing bacterium (Bonny et al. 2013).

Another important example of cell-scale waves is actin waves (Allard & Mogilner 2013; Alt & Tranquillo 1995; Inagaki & Katsuno 2017; Vicker 2002), which propagate due to diffusion or polymerization (Bretschneider et al. 2009). In big oocytes of several animal species, for example frog (Hara et al. 1980) and starfish (Hamaguchi & Hiramoto 1978), waves of actin propagate at the surface of the egg (surface contraction waves or SCW) in association with the cell cycle. The contraction is based on RhoA-GTP (Bement et al. 2015) that leads to actomyosin contractility (Bischof et al. 2017). SCW propagate in interphase, when Cyclin-dependent kinase 1 (Cdk1) is inhibited (Bement et al. 2015), starting at the point of lowest Cdk1 concentration (Bischof et al. 2017; Wigbers et al. 2021). Cdk1 inhibits the RhoGEF Ect2, such that a gradient of Cdk1 leads to a trigger wave of Ect2, itself leading to a traveling wave of RhoA-GTP (Wigbers et al. 2021) (Figure 3B). Negative feedback shaping the RhoA waveform comes from components downstream of RhoA (Bischof et al. 2017), for example actin itself (Bement et al. 2015). Interestingly, when Ect2 is overexpressed, spiral waves of RhoA-GTP appear (Bement et al. 2015), revealing the excitable nature of the system (Figure 3B).

A possible function for surface contraction waves could be to synchronize mitosis in big cells like *Xenopus* (1.2mm) (Chang & Ferrell Jr 2013), or to sense the shape of the cell (Wigbers et al. 2021). Indeed, in systems with multiple nuclei dividing and without membrane separation, mitosis is coordinated by waves of Cdk1, for example in *Xenopus* egg extracts (Chang & Ferrell

Jr 2013) and the *Drosophila* syncytial embryo (Deneke et al. 2016; Vergassola et al. 2018). In *Drosophila*, mitotic waves are kinematic waves induced by a Cdk1 trigger wave (Deneke et al. 2016) (Figure 3C), though an alternative model of Cdk1 wave was recently proposed (Vergassola et al. 2018).

An important function of waves is to propagate information faster and over longer distances than can be accomplished by diffusion alone (Gelens et al. 2014). Most notably, action potential, the propagation of a change in voltage across a membrane due to opening of ion channels (Hodgkin & Huxley 1952), propagates as a trigger wave in neurons at a speed of 100 m/s over meters (Heimburg & Jackson 2007). Similarly, waves of free cytosolic calcium ions based on phospho-lipid signaling, reach speeds up to 30 m/s (reviewed in (Jaffe 2008)). At the tissue scale, calcium waves can cover 20 cells/s (Koenigsberger et al. 2010). Calcium waves are important for muscle contraction, and are also present in developing tissues such as the fly ommatidia (Ready & Chang 2021) and wing disk (Balaji et al. 2017).

Progress in time-resolved microscopy of developing organisms is revealing that spatial tissue patterns often emerge through wave-like patterns. For example, the patterning underlying adult vertebrate formation (Pourquié 2003), and insect segmentation (El-Sherif et al. 2012, 2014) rely on waves of gene expression. Another example is the *Drosophila* crystal-like eye structure, which is made of elementary units, the ommatidia, with a geometrical arrangement. Ommatidia are formed progressively, following a wave front of *hedgehog* and *decapentaplegic* gene expression that sweeps across the eye disk surface (Heberlein et al. 1993; Ready et al. 1976). This phenomenon has been modeled as a 'switch-and-template' cellular model, with cell-autonomous bistability and separation of time- and length- scales as key ingredients (Gavish et al. 2016; Lubensky et al. 2011).

At an even larger scale, groups of organisms can also form oscillating wave patterns, such as groups of the amoeba *Dictyostelium* that display oscillations, waves, and spirals of cAMP (Pálsson & Cox 1996).

3. SPONTANEOUS FORMATION OF MECHANOCHEMICAL PATTERNS

The processes that we have discussed so far involve only interactions between chemical species. However, mechanics is known to play an important role in biology, from active transport of matter by molecular motors, to large-scale flows within the cytoplasm, to the folding of tissues during morphogenesis (Hannezo & Heisenberg 2019). In this section, we focus on how mechanical forces can play a role in pattern formation within biological systems and how this compares to and interacts with self-organization involving only chemical interactions.

3.1. Theory of mechanically- and mechanochemically- formed spatial patterns

To consider the impact of mechanics on the flow of a medium, one must consider what different forces are acting in the system. Many biological systems contain an actomyosin cortex composed of a cytoskeletal meshwork of actin filaments that are crosslinked by myosin motors. By consuming ATP, the myosin motors can move along the actin filaments, thereby generating contractile stresses. Because of this underlying active, contractile cortex, these systems can be considered as viscous active fluids (Bois et al. 2011). In such systems, the relevant forces arise due to the passive viscous stress (σ_p), the active stress driven by myosin (σ_a), and any external forces in play such as friction. The force balance given by these elements is (Bois et al. 2011):

$$\nabla \cdot \sigma = \gamma v \tag{2}$$

where $\sigma \equiv \sigma_p + \sigma_a$ is the total stress, γ is the friction coefficient, v is velocity of the medium. This equation yields the intuitive result that flows are directed towards regions of high stress such as can be generated by high myosin concentration. These flows will carry with them (or advect) any objects that are contained in the medium.

We can now compare the impact of advection with that of diffusion, which drives the formation of patterns in purely chemical systems. These two processes have opposite effects, with advection concentrating material to regions of high stress and diffusion dispersing any non-uniformity in concentration. Diffusion can produce large effects locally, but cannot propagate information quickly or over large length scales (Gelens et al. 2014). On the contrary, forces generated by stress can travel a million times faster than diffusion, and over long distances (Howard et al. 2011).

Due to their opposing impacts, interesting effects can occur when advection and diffusion are considered together. Adding advection to the reaction-diffusion model gives an updated version of Equation 1 (Bois et al. 2011; Gross et al. 2017):

$$\partial C_i/\partial t = -\nabla \cdot (vC_i) + D_i \nabla^2 C_i + R_i(C_1, \ldots C_n) \quad (3)$$

where v is the advection velocity, which is calculated using Equation 2. Advection of components of active stress regulation, such as myosin itself, works as a positive feedback that amplifies local density fluctuations and causes instability. Viscosity, friction and diffusion work as long-range inhibitors of such instabilities. Temporarily removing the reaction terms gives a set of equations where self-reinforcing concentration of myosin is balanced by the stabilizing effects of viscosity, friction, and diffusion (Figure 4A) (Bois et al. 2011).

Advection is not the only mechanical effect that can play a role in pattern formation. While biological systems can generally be treated as viscous systems, in certain circumstances it can be important to consider the contributions of elasticity (Özkaya et al. 2017). Elasticity can be considered theoretically by including contributions of the elastic modulus to the stress tensor (σ) given in Equation 2 (Murray & Oster 1984) and having v represent the elastic displacement field instead of the advection velocity (Gross et al. 2017). Elasticity can work as a long-range inhibitor of pattern formation since a stiffer medium will reduce the displacement field (Figure 4B).

Biological systems seldom use mechanics alone, instead relying on the interplay between chemical and mechanical effects (Mammoto & Ingber 2010). In addition to causing flow, which impacts the localization of contractile species, stresses in a system can lead to advection of other, passive molecules. These passive molecules, while not creating stress in and of themselves, can alter the mechanics of the system, thereby creating complex feedback loops (Gross et al. 2017).

3.2. Spatial mechanochemical patterns in biological systems

The importance of mechanics in biological pattern formation has been shown experimentally in many systems. For example, the ability for contractility to act as a self-reinforcing activator with friction acting as its inhibitor has been demonstrated in the formation of actin rings in the *Drosophila* trachea (Hannezo et al. 2015). The authors model the trachea using a system of equations equivalent to those given by Equations 2 and 3 with the addition of a term related to actin turnover. Solving these equations gives a wavelength for rings of actin that encircle the trachea. They show that the predicted wavelength approximates that seen experimentally, and

that by tuning the myosin contractility and the friction coefficient of the system they can change the spacing of the rings as predicted (Figure 4C).

The effects of elasticity on pattern formation of fibroblasts and mesenchymal cells has been studied for a long time (Figure 4D) (Harris et al. 1981, 1984; Murray et al. 1983). In these systems, contractility acts to provide local activation while tissue stiffness due to elasticity acts as an inhibitor (Oster & Murray 1989). More recently, experiments have been performed that show a similar interplay between local contractile forces and long-range elastic forces during the formation of follicle patterns in avian skin (Shyer et al. 2017). The pattern of follicle primordia changes in response to changes in the stiffness and contractility of avian skin explants (Figure 4E).

The interplay between mechanics and chemistry has also been shown to be sufficient for pattern formation in simulations (Brinkmann et al. 2018; Mercker et al. 2016; Veerman et al. 2021), and in several experimental processes at the cell or tissue scales. In keratocytes and neutrophil cells, membrane tension generated by actin polymerization at the leading edge provides a long-range inhibition to Rac activity. This enables polarization of the front of migrating cells and prevents secondary fronts from appearing (Houk et al. 2012) (Figure 4F). A similar mechanism operates at the tissue scale; the formation of the avian primitive streak occurs because mechanical tension inhibits constriction over a long range, ensuring the development of a single constriction site (Figure 4G) (Caldarelli et al. 2021). Other examples include the establishment of polarity in the *Caenorhabditis elegans* embryo (Gross et al. 2019; Mayer et al. 2010), *Hydra* regeneration (Mercker et al. 2015), and myosin patterns in stress fibers and sarcomeres (Dasbiswas et al. 2018).

3.3. Temporal patterns

We saw in Section 2 that non-linearity and delayed negative feedback loops in chemical reactions can generate oscillations. Mechanical forces or deformation, sensed by molecules, can also cause delayed feedback in a chemical system, causing it to oscillate. The delay can be a direct consequence of the addition of new intermediate mechanochemical reactions. In addition, mechanical properties such as advection and elasticity, can feed directly back into a system, as discussed above. For example, collections of molecular motors can generate oscillations of cytoskeletal polymers like microtubules (Beta & Kruse 2017). One striking example of oscillations in the cytoskeleton is the case of actomyosin pulses.

Oscillations in actin and non-muscle Myosin II (MyoII) concentration occur at the cortex of cells, accompanied by cortical contractions (most recently reviewed in (Miao & Blankenship 2020)). Such oscillations were first observed in the *C.elegans* cortex (Munro et al. 2004). It is now clear that this is a conserved feature, present in the gastrulating *Drosophila* embryo (Martin et al. 2009; Rauzi et al. 2010; Solon et al. 2009), the cortex of the mouse blastocyst (Maître et al. 2015), and the *Xenopus* mesoderm (Kim & Davidson 2011). Cortical MyoII pulses are involved in morphogenetic processes, such as apical cell constriction (Martin et al. 2009; Solon et al. 2009), cell intercalation (Collinet et al. 2015; Kim & Davidson 2011; Rauzi et al. 2010; Yu & Fernandez-Gonzalez 2016), tissue elongation (Alégot et al. 2018; He et al. 2010), wound healing (Antunes et al. 2013; Razzell et al. 2014), blastocyst compaction (Maître et al. 2015), cell delamination (An et al. 2017; Michel & Dahmann 2020; Simões et al. 2017), and partner-cell matching (Zhang et al. 2020).

In some cases, oscillations in MyoII activation happen downstream of Rho signaling, with Rho-GTP oscillating independently (Michaux et al. 2018; Nishikawa et al. 2017). The pulse of Rho-GTP is initiated by positive feedback of RhoA-GTP onto itself (Michaux et al. 2018), and

terminated by delayed negative feedback arising from F-actin accumulation and subsequent concentration of the RhoA GTPase-activating protein RGA-3/4, an inhibitor of RhoA that is recruited by F-actin (Michaux et al. 2018). In other cases, mechanical feedback from the contractility itself is necessary for increased MyoII at cell junctions (Fernandez-Gonzalez et al. 2009), and for medial apical pulses (Munjal et al. 2015) (Figure 5A). Such feedback could come from a mechanosensitive motor binding/unbinding rate (Greenberg et al. 2016; Hayakawa et al. 2011; Kovács et al. 2007; Ren et al. 2009), from other mechanosensitive pathways (e.g. calcium signaling (Kapustina et al. 2008)), or from advection of positive regulators due to cortical flows (Munjal et al. 2015).

Theoretical work has shown that it is possible to obtain oscillations and limit cycles (Section 2.3) based on mechanical feedback (Dierkes et al. 2014; Koride et al. 2014; Kumar et al. 2014; Machado et al. 2014). For example, an active elastomer model with strain-induced unbinding of MyoII can account for experimentally observed MyoII pulses in *Drosophila* (Banerjee et al. 2017). These models can also be extended to include the associated Rho pulses (Staddon et al. 2021). Theoretical work can help identify the importance of mechanics in such systems.

3.4. Spatiotemporal patterns

As in chemical systems, adding spatial coupling to the mechanochemical oscillations described above can lead to wave propagation. More often than not, biological waves involve both chemical and mechanical elements.

One method for wave formation is for the positive feedback loop to be mechanical. Mechanochemical models show that actomyosin pulses can propagate in space as waves

(Banerjee et al. 2017; Dierkes et al. 2014; Kumar et al. 2014) due to diffusion. In this case, there is chemical spatial coupling based on diffusion, and a mechanical positive feedback loop based on advection. Such actomyosin waves can be seen within *Drosophila* amnioserosa cells (Blanchard et al. 2010).

Alternatively, the spatial coupling can be mechanical. This is the case in actin waves that form in migrating cells. In particular, the tip of an actin-rich lamellipodium undergoes cycles of protrusion and retraction that propagate as a wave (Abercrombie et al. 1970; Allard & Mogilner 2013; Giannone et al. 2004; Inagaki & Katsuno 2017; Ryan et al. 2012b; Weiner et al. 2007). Protrusion-retraction can be modeled as an excitable system (Ryan et al. 2012a) though it is not clear what mechanism provides spatial coupling. One possibility is that the wave is set by coupling from diffusion and a chemical positive feedback, such as a RhoA-RhoGDI pacemaker (Machacek et al. 2009; Tkachenko et al. 2011). However, spatial coupling could alternatively arise from mechanical forces or deformation since the protrusion-retraction cycle has been linked to MyoII contractility (Driscoll et al. 2012; Giannone et al. 2007). Curvature-sensing proteins could also play a role in actin protrusion waves (Peleg et al. 2011; Shlomovitz & Gov 2007). The presence of convex membrane proteins that activate actin polymerization, together with MyoII contractility, could theoretically give rise to membrane ruffles or waves. MyoII contractility bends the membrane inward where actin is dense, creating two ‘shoulders’ of opposite curvature on either side of the patch. The membrane proteins diffuse to these shoulders due to their favored curvature, increasing actin and myosin concentration and leading to a wave (Shlomovitz & Gov 2007). Such wave-like deformations may have a role in cell motility: deformations produced by actin waves in migrating cells could be more efficient at probing the environment (Wigbers et al. 2021), or could help avoid obstacles (Weiner et al. 2007) and crawl when adhesion is low (Allard & Mogilner 2013; Driscoll et al. 2012).

At the tissue scale, spatial coupling cannot be provided by diffusion or polymerization, since the cell membrane acts as a barrier. We therefore need to consider what physical mechanisms might play a role in such systems. In principle, active mechanical stress in a tissue propagates, causing deformation at a distance. This deformation can then be sensed by a dedicated cellular chemical pathway, triggering a positive feedback. We can see such phenomena in expansion-contraction waves in expanding or colliding epithelial monolayers (Rodríguez-Franco et al. 2017; Serra-Picamal et al. 2012; Tlili et al. 2018). Mechanical expansion-contraction waves are associated with chemical ERK waves that propagate and orient migration (Aoki et al. 2017). In a given cell, ERK induces contractility, subsequently stretching its neighbors in the plane of the tissue. Stretch is then transduced into ERK activity via epidermal growth factor receptor activation, resulting in a wave (Boocock et al. 2020; Hino et al. 2020) (Figure 5B). ERK waves associated with deformation have also been observed in vivo during zebrafish scale regeneration (De Simone et al. 2021).

More complex tissue geometries can lead to different forms of mechanical coupling in tissues. In ascidian neural tube closure, a wave of Myosin activation is observed along the junctions of the zippering neural tube, just ahead of the zipper (Hashimoto et al. 2015). The mechanism responsible for spatial coupling is unknown but could arise from the geometric effect of bringing neighboring cells into contact across the midline due to contraction, leading to the propagation of activation. Tissues can also fold and deform in three dimensions. During *Drosophila* gastrulation, a transcription-independent wave of MyoII activation propagates from cell to cell in the dorsal region of the embryo (Bailles et al. 2019) (Figure 5C). The wave depends on MyoII contractility and integrin-based adhesion to the surrounding vitelline membrane. The spatial coupling is provided by MyoII-induced tissue invagination that

compresses distant cells against the vitelline membrane, creating integrin attachment (Figure 5C).

What could be the role of tissue-scale waves? Motion occurring in a wave-like pattern could be required for proper morphogenesis, as a progressive deformation is more efficient than a synchronized one and limits mechanical stress accumulation. During *Drosophila* placode invagination, the cells invaginate as a wave (Nishimura et al. 2007), which has been hypothesized to facilitate the bending of the epithelium compared to a gradient-based mechanism (Ogura et al. 2018). A wave could also be useful for forming precise and defect-free cellular patterns. In *Drosophila* ommatidia, the morphogenetic wave may use one row of ommatidia as a mechanical template for the next (Gallagher et al. 2021). In flighted birds, a wave of cellular density controls the highly-ordered formation of feathers (Ho et al. 2019).

4. DISCUSSION

Patterns are ubiquitous in the living world. They occur across scales, from within cells to between organisms. They manifest in space and time and rely on a wide range of chemical and mechanical processes. Therefore, one may doubt that general principles of pattern formation could exist. Indeed, the past few decades have revealed a vast diversity of molecules and mechanisms that can produce such patterns. When generality has been suggested, it is mainly the conservation of genes and proteins that has been emphasized rather than the logic of how patterns emerge. Here, we focus on such a generalized logic and argue that there are principles of pattern formation that transcend the specifics of how patterns are created. We focus on a few such principles associated with spatial and temporal patterns as identified with mathematical models and observed in real biological systems.

Chemical and mechanochemical spatial patterns have common features (Figures 1 and 4). At their core, they require a local process that amplifies a fluctuation, coupled to a non-local process that inhibits at a distance. In chemical systems (Figure 1), this may arise from a positive feedback on one of the components, at least one negative feedback, and diffusion, which is linear and non-local. The vast majority of two- or three- node networks that produce Turing-like patterns possess such properties (Scholes et al. 2019). In mechanical systems (Figure 4), positive feedback is usually associated with contractility, and mechanical long-range inhibition appears as a result of the elasticity or viscosity of the medium. Temporal patterns such as oscillations can arise from delayed negative feedback in systems which contain positive feedback (Figure 2). When this is combined with spatial coupling mechanisms arising from diffusion of molecules (Figure 3), or mechanical forces (Figure 5), waves can emerge that propagate across a cell or tissue.

As we have shown in this review, self-organized spatial and temporal patterns rely on effective parameters (eg. diffusivity, friction, reaction kinetics) and processes (eg. positive feedback loop, or long-range inhibition) that dictate the system's behavior. Several or many molecules may be associated with each process in vivo, but in the end understanding the logic of the systems relies on the knowledge of few such processes and effective parameters.

This simplicity can come at a cost; while excitable systems are inherently robust due to their positive feedback, spatial Turing patterns are not very robust. Many networks that are able to form Turing patterns, can only do so for a small range of parameters (Maini et al. 2012; Scholes et al. 2019). However, in nature, spatial patterns must be reproducible. How can such systems deal with this sensitivity in the face of noisy and variable conditions? In vivo, self-organized patterns are often canalized by external biases that define the initial and boundary conditions

through three modules of information: biochemistry, mechanics, and geometry (Collinet & Lecuit 2021). Indeed, patterns build upon other patterns during the lifetimes of cells and embryos. For example, the *Drosophila* notum sensory organ precursors are formed from a combination of a pre-established gradient and lateral inhibition (Cohen et al. 2010; Corson et al. 2017). In addition, it has been shown that the addition of boundary conditions and growth to tissues can have profound effects on the patterns and it has been suggested that these effects can serve to make pattern formation more robust (Barrio et al. 1999; Maini et al. 2012). It would be interesting to experimentally explore this possibility in the future. Using in vitro systems, such as gastruloids and organoids, will help disentangle the contribution of prepatterning and self-organization in development (Etoc et al. 2016; Gjorevski et al. 2022; Schauer et al. 2020; Simunovic et al. 2019; Warmflash et al. 2014).

Whole embryos and synthetic systems both provide a rich context to study the role of chemical, mechanical, and geometric constraints on the self-organization of patterns. The combination of experimental systems and mathematical models sets the stage for the quest of principles underlying the dynamic organization of cells and tissues into a functional whole.

DISCLOSURE STATEMENT

The authors declare no competing interests.

ACKNOWLEDGMENTS

The authors thank all members of the Lecuit group for stimulating discussions and Annemarie Lellouch, Claudio Collinet, Matthias Merkel and Alexander Erlich for useful feedback on this manuscript. This review emerged from a lecture series at the Collège de France in 2018. E.G.

is supported by the ERC grant SelfControl #788308. T.L. is supported by the Collège de France. A.B. is supported by the European Molecular Biology Organization (EMBO) under award number ALTF 785-2020.

LITERATURE CITED

Abercrombie M, Heaysman JEM, Pegrum SM. 1970. The locomotion of fibroblasts in culture I. Movements of the leading edge. *Exp Cell Res*. 59(3):393–98

Alégot H, Pouchin P, Bardot O, Mirouse V. 2018. Jak-Stat pathway induces Drosophila follicle elongation by a gradient of apical contractility. *eLife*. 7:e32943

Allard J, Mogilner A. 2013. Traveling waves in actin dynamics and cell motility. *Curr Opin Cell Biol*. 25(1):107–15

Alt W, Tranquillo RT. 1995. Basic morphogenetic system modeling shape changes of migrating cells: how to explain fluctuating lamellipodial dynamics. *J Biol Syst*. 03(04):905–16

An Y, Xue G, Shaobo Y, Mingxi D, Zhou X, et al. 2017. Apical constriction is driven by a pulsatile apical myosin network in delaminating Drosophila neuroblasts. *Development*. 144(12):2153–64

Antunes M, Pereira T, Cordeiro JV, Almeida L, Jacinto A. 2013. Coordinated waves of actomyosin flow and apical cell constriction immediately after wounding. *J Cell Biol*. 202(2):365–79

Aoki K, Kondo Y, Naoki H, Hiratsuka T, Itoh RE, Matsuda M. 2017. Propagating wave of ERK activation orients collective cell migration. *Dev Cell*. 43(3):305-317.e5

Bailles A, Collinet C, Philippe J-M, Lenne P-F, Munro E, Lecuit T. 2019. Genetic induction and mechanochemical propagation of a morphogenetic wave. *Nature*. 572(7770):467–73

Balaji R, Bielmeier C, Harz H, Bates J, Stadler C, et al. 2017. Calcium spikes, waves and oscillations in a large, patterned epithelial tissue. *Sci Rep*. 7(1):42786

Banerjee DS, Munjal A, Lecuit T, Rao M. 2017. Actomyosin pulsation and flows in an active elastomer with turnover and network remodeling. *Nat Commun*. 8(1):1121

Bargiello TA, Jackson FR, Young MW. 1984. Restoration of circadian behavioural rhythms by gene transfer in Drosophila. *Nature*. 312(5996):752–54

Bargiello TA, Young MW. 1984. Molecular genetics of a biological clock in Drosophila. *Proc Natl Acad Sci U S A*. 81(7):2142–46

Barr I. 2017. Turing Patterns

Barrio RA, Varea C, Aragon JL. 1999. A two-dimensional numerical study of spatial pattern formation in interacting Turing systems. *Bull Math Biol*. 61(3):483–505

Bement WM, Leda M, Moe AM, Kita AM, Larson ME, et al. 2015. Activator–inhibitor coupling between Rho signalling and actin assembly makes the cell cortex an excitable medium. *Nat Cell Biol*. 17(11):1471–83

Bender A, Pringle JR. 1989. Multicopy suppression of the *cdc24* budding defect in yeast by *CDC42* and three newly identified genes including the *ras*-related gene *RSR1*. *Proc Natl Acad Sci U S A*. 86(24):9976–80

Beta C, Kruse K. 2017. Intracellular oscillations and waves. *Annu Rev Condens Matter Phys*. 8(1):239–64

Bischof J, Brand CA, Somogyi K, Májer I, Thome S, et al. 2017. A cdk1 gradient guides surface contraction waves in oocytes. *Nat Commun*. 8(1):849

Blanchard GB, Murugesu S, Adams RJ, Martinez-Arias A, Gorfinkiel N. 2010. Cytoskeletal dynamics and supracellular organisation of cell shape fluctuations during dorsal closure. *Development*. 137(16):2743–52

Bois JS, Jülicher F, Grill SW. 2011. Pattern formation in active fluids. *Phys Rev Lett*.

106(2):028103

Bonny M, Fischer-Friedrich E, Loose M, Schwille P, Kruse K. 2013. Membrane Binding of MinE Allows for a Comprehensive Description of Min-Protein Pattern Formation. *PLoS Comp Biol*. 9(12):e1003347

Boocock D, Hino N, Ruzickova N, Hirashima T, Hannezo E. 2020. Theory of mechano-chemical patterning and optimal migration in cell monolayers

Borgqvist J, Malik A, Lundholm C, Logg A, Gerlee P, Cvijovic M. 2021. Cell polarisation in a bulk-surface model can be driven by both classic and non-classic Turing instability. *NPJ Syst Biol Appl*. 7(1):1–10

Bretschneider T, Anderson K, Ecke M, Müller-Taubenberger A, Schroth-Diez B, et al. 2009. The three-dimensional dynamics of actin waves, a model of cytoskeletal self-organization. *Biophys J*. 96(7):2888–2900

Brinkmann F, Mercker M, Richter T, Marciniak-Czochra A. 2018. Post-Turing tissue pattern formation: Advent of mechanochemistry. *PLoS Comput Biol*. 14(7):e1006259

Buck J, Buck E. 1968. Mechanism of rhythmic synchronous flashing of fireflies. *Science*. 159(3821):1319–27

Buijs RM, Kalsbeek A. 2001. Hypothalamic integration of central and peripheral clocks. *Nat Rev Neurosci*. 2(7):521–26

Cai L, Dalal CK, Elowitz MB. 2008. Frequency-modulated nuclear localization bursts coordinate gene regulation. *Nature*. 455(7212):485–90

Caldarelli P, Chamolly A, Alegria-Prévot O, Gros J, Corson F. 2021. Self-organized tissue mechanics underlie embryonic regulation. *bioRxiv*. doi:10.1101/2021.10.08.463661

Ceriani MF, Darlington TK, Staknis D, Más P, Petti AA, et al. 1999. Light-dependent sequestration of TIMELESS by CRYPTOCHROME. *Science*. 285(5427):553–56

Chang JB, Ferrell Jr JE. 2013. Mitotic trigger waves and the spatial coordination of the

Xenopus cell cycle. *Nature*. 500(7464):603–7

Chant J, Herskowitz I. 1991. Genetic control of bud site selection in yeast by a set of gene products that constitute a morphogenetic pathway. *Cell*. 65:1203–12

Cohen M, Georgiou M, Stevenson NL, Miodownik M, Baum B. 2010. Dynamic filopodia transmit intermittent Delta-Notch signaling to drive pattern refinement during lateral inhibition. *Dev Cell*. 19(1):78–89

Collinet C, Lecuit T. 2021. Programmed and self-organized flow of information during morphogenesis. *Nat Rev Mol Cell Biol*. 22(4):245–65

Collinet C, Rauzi M, Lenne P-F, Lecuit T. 2015. Local and tissue-scale forces drive oriented junction growth during tissue extension. *Nat Cell Biol*. 17(10):1247–58

Corson F, Couturier L, Rouault H, Mazouni K, Schweisguth F. 2017. Self-organized Notch dynamics generate stereotyped sensory organ patterns in Drosophila. *Science*. 356(6337):eaai7407

Dasbiswas K, Hu S, Schnorrer F, Safran SA, Bershadsky AD. 2018. Ordering of myosin II filaments driven by mechanical forces: experiments and theory. *Philos Trans R Soc Lond B Biol Sci*. 373(1747):20170114

de Boer PAJ, Crossley RE, Rothfield LI. 1989. A division inhibitor and a topological specificity factor coded for by the minicell locus determine proper placement of the division septum in E. coli. *Cell*. 56(4):641–49

De Simone A, Evanitsky MN, Hayden L, Cox BD, Wang J, et al. 2021. Control of osteoblast regeneration by a train of Erk activity waves. *Nature*. 590(7844):129–33

Delacour D, Salomon J, Robine S, Louvard D. 2016. Plasticity of the brush border — the yin and yang of intestinal homeostasis. *Nat Rev Gastroenterol Hepatol*. 13(3):161–74

Deneke VE, Melbinger A, Vergassola M, Di Talia S. 2016. Waves of Cdk1 activity in S phase synchronize the cell cycle in Drosophila embryos. *Dev Cell*. 38(4):399–412

Depasquale JA. 2018. Actin microridges. *Anat Rec*. 301(12):2037–50

Dierkes K, Sumi A, Solon J, Salbreux G. 2014. Spontaneous oscillations of elastic contractile materials with turnover. *Phys Rev Lett*. 113(14):148102

Driscoll MK, McCann C, Kopace R, Homan T, Fourkas JT, et al. 2012. Cell shape dynamics: From waves to migration. *PLoS Comput Biol*. 8(3):e1002392

Economou AD, Ohazama A, Porntaveetus T, Sharpe PT, Kondo S, et al. 2012. Periodic stripe formation by a Turing mechanism operating at growth zones in the mammalian palate. *Nat Genet*. 44(3):348–51

El-Sherif E, Averof M, Brown SJ. 2012. A segmentation clock operating in blastoderm and germband stages of Tribolium development. *Development*. 139(23):4341–46

El-Sherif E, Zhu X, Fu J, Brown SJ. 2014. Caudal regulates the spatiotemporal dynamics of pair-rule waves in Tribolium. *PLoS Genet*. 10(10):e1004677

Emery P, So WV, Kaneko M, Hall JC, Rosbash M. 1998. CRY, a Drosophila clock and light-regulated cryptochrome, is a major contributor to circadian rhythm resetting and photosensitivity. *Cell*. 95(5):669–79

Eom DS, Bain EJ, Patterson LB, Grout ME, Parichy DM. 2015. Long-distance communication by specialized cellular projections during pigment pattern development and evolution. *eLife*. 4:e12401

Ermentrout B. 1991. Stripes or spots? Nonlinear effects in bifurcation of reaction—diffusion equations on the square. *Proc R Soc Lond A Math Phys Sci*. 434(1891):413–17

Etoc F, Metzger J, Ruzo A, Kirst C, Yoney A, et al. 2016. A balance between secreted inhibitors and edge-sensing controls gastruloid self-organization. *Dev Cell*. 39(3):302–15

Evans T, Rosenthal ET, Youngblom J, Distel D, Hunt T. 1983. Cyclin: A protein specified by maternal mRNA in sea urchin eggs that is destroyed at each cleavage division. *Cell*.

33(2):389–96

Fernandez-Gonzalez R, Simoes S de M, Röper J-C, Eaton S, Zallen JA. 2009. Myosin II dynamics are regulated by tension in intercalating cells. *Dev Cell*. 17(5):736–43

Ferrell JE, Tsai TY-C, Yang Q. 2011. Modeling the cell cycle: Why do certain circuits oscillate? *Cell*. 144(6):874–85

FitzHugh R. 1961. Impulses and physiological states in theoretical models of nerve membrane. *Biophys J*. 1(6):445–66

Frohnhöfer HG, Krauss J, Maischein H-M, Nüsslein-Volhard C. 2013. Iridophores and their interactions with other chromatophores are required for stripe formation in zebrafish. *Development*. 140(14):2997–3007

Gallagher KD, Mani M, Carthew RW. 2021. Emergence of a geometric pattern of cell fates from tissue-scale mechanics in the Drosophila eye. *bioRxiv*. doi:10.1101/2021.07.14.452386

Gavish A, Shwartz A, Weizman A, Schejter E, Shilo B-Z, Barkai N. 2016. Periodic patterning of the Drosophila eye is stabilized by the diffusible activator Scabrous. *Nat Commun*. 7(1):1–10

Gelens L, Anderson GA, Ferrell JE. 2014. Spatial trigger waves: positive feedback gets you a long way. *Mol Biol Cell*. 25(22):3486–93

Gerisch G, Fromm H, Huesgen A, Wick U. 1975. Control of cell-contact sites by cyclic AMP pulses in differentiating Dictyostelium cells. *Nature*. 255(5509):547–49

Giannone G, Dubin-Thaler BJ, Döbereiner H-G, Kieffer N, Bresnick AR, Sheetz MP. 2004. Periodic lamellipodial contractions correlate with rearward actin waves. *Cell*. 116(3):431–43

Giannone G, Dubin-Thaler BJ, Rossier O, Cai Y, Chaga O, et al. 2007. Lamellipodial actin mechanically links myosin activity with adhesion-site formation. *Cell*. 128(3):561–75

Gierer A, Meinhardt H. 1972. A theory of biological pattern formation. *Kybernetik*. 12(1):30–39

Gjorevski N, Nikolaev M, Brown TE, Mitrofanova O, Brandenberg N, et al. 2022. Tissue geometry drives deterministic organoid patterning. *Science*. 375(6576):eaaw9021

Goryachev AB, Pokhilko AV. 2008. Dynamics of Cdc42 network embodies a Turing-type mechanism of yeast cell polarity. *FEBS Lett.* 582(10):1437–43

Gray P, Scott SK. 1984. Autocatalytic reactions in the isothermal, continuous stirred tank reactor: Oscillations and instabilities in the system A + 2B → 3B; B → C. *Chem Eng Sci*. 39(6):1087–97

Greenberg MJ, Arpağ G, Tüzel E, Ostap EM. 2016. A perspective on the role of myosins as mechanosensors. *Biophys J*. 110(12):2568–76

Gross P, Kumar KV, Goehring NW, Bois JS, Hoege C, et al. 2019. Guiding self-organized pattern formation in cell polarity establishment. *Nat Phys*. 15(3):293–300

Gross P, Kumar KV, Grill SW. 2017. How active mechanics and regulatory biochemistry combine to form patterns in development. *Annu Rev Biophys*. 46:337–56

Halatek J, Brauns F, Frey E. 2018. Self-organization principles of intracellular pattern formation. *Philos Trans R Soc Lond B Biol Sci*. 373(1747):20170107

Hamaguchi MS, Hiramoto Y. 1978. Protoplasmic movement during polar-body formation in starfish oocytes. *Exp Cell Res*. 112(1):55–62

Hannezo E, Dong B, Recho P, Joanny J-F, Hayashi S. 2015. Cortical instability drives periodic supracellular actin pattern formation in epithelial tubes. *Proc Natl Acad Sci U S A*. 112(28):8620–25

Hannezo E, Heisenberg C-P. 2019. Mechanochemical feedback loops in development and disease. *Cell*. 178(1):12–25

Hara K, Tydeman P, Kirschner M. 1980. A cytoplasmic clock with the same period as the

division cycle in Xenopus eggs. *Proc Natl Acad Sci U S A*. 77(1):462–66

Harris AK, Stopak D, Warner P. 1984. Generation of spatially periodic patterns by a mechanical instability: a mechanical alternative to the Turing model. *J Embryol Exp Morphol*. 80:1–20

Harris AK, Stopak D, Wild P. 1981. Fibroblast traction as a mechanism for collagen morphogenesis. *Nature*. 290(5803):249–51

Hashimoto H, Robin FB, Sherrard KM, Munro EM. 2015. Sequential contraction and exchange of apical junctions drives zippering and neural tube closure in a simple chordate. *Dev Cell*. 32(2):241–55

Hayakawa K, Tatsumi H, Sokabe M. 2011. Actin filaments function as a tension sensor by tension-dependent binding of cofilin to the filament. *J Cell Biol*. 195(5):721–27

He L, Wang X, Tang HL, Montell DJ. 2010. Tissue elongation requires oscillating contractions of a basal actomyosin network. *Nat Cell Biol*. 12(12):1133–42

Heberlein U, Wolff T, Rubin GM. 1993. The TGFβ homolog dpp and the segment polarity gene hedgehog are required for propagation of a morphogenetic wave in the Drosophila retina. *Cell*. 75(5):913–26

Heimburg T, Jackson AD. 2007. On the action potential as a propagating density pulse and the role of anesthetics. *Biophys Rev Lett*. 02(01):57–78

Heyde A, Guo L, Jost C, Theraulaz G, Mahadevan L. 2021. Self-organized biotectonics of termite nests. *Proc Natl Acad Sci U S A*. 118(5):e2006985118

Hino N, Rossetti L, Marín-Llauradó A, Aoki K, Trepat X, et al. 2020. ERK-mediated mechanochemical waves direct collective cell polarization. *Dev Cell*. 53(6):646-660.e8

Hiscock TW, Megason SG. 2015. Mathematically guided approaches to distinguish models of periodic patterning. *Development*. 142(3):409–19

Ho WKW, Freem L, Zhao D, Painter KJ, Woolley TE, et al. 2019. Feather arrays are patterned by interacting signalling and cell density waves. *PLOS Biology*. 17(2):e3000132

Hodgkin AL, Huxley AF. 1952. A quantitative description of membrane current and its application to conduction and excitation in nerve. *J Physiol*. 117(4):500–544

Houk AR, Jilkine A, Mejean CO, Boltyanskiy R, Dufresne ER, et al. 2012. Membrane tension maintains cell polarity by confining signals to the leading edge during neutrophil migration. *Cell*. 148(1):175–88

Howard J, Grill SW, Bois JS. 2011. Turing's next steps: the mechanochemical basis of morphogenesis. *Nat Rev Mol Cell Biol*. 12(6):392–98

Howell AS, Jin M, Wu C-F, Zyla TR, Elston TC, Lew DJ. 2012. Negative feedback enhances robustness in the yeast polarity establishment circuit. *Cell*. 149(2):322–33

Hu Z, Lutkenhaus J. 1999. Topological regulation of cell division in Escherichia coli involves rapid pole to pole oscillation of the division inhibitor MinC under the control of MinD and MinE. *Mol Microbiol*. 34(1):82–90

Huang C-H, Tang M, Shi C, Iglesias PA, Devreotes PN. 2013. An excitable signal integrator couples to an idling cytoskeletal oscillator to drive cell migration. *Nat Cell Biol*. 15(11):1307–16

Iglesias PA, Devreotes PN. 2008. Navigating through models of chemotaxis. *Current Opinion in Cell Biology*. 20(1):35–40

Inagaki N, Katsuno H. 2017. Actin waves: Origin of cell polarization and migration? *Trends Cell Biol*. 27(7):515–26

Irazoqui JE, Gladfelter AS, Lew DJ. 2003. Scaffold-mediated symmetry breaking by Cdc42p. *Nat Cell Biol*. 5(12):1062–70

Jaffe LF. 2008. Calcium waves. *Philos Trans R Soc Lond B Biol Sci*. 363(1495):1311–17

Kapustina M, Weinreb GE, Costigliola N, Rajfur Z, Jacobson K, Elston TC. 2008. Mechanical and biochemical modeling of cortical oscillations in spreading cells. *Biophysis J*. 94(12):4605–20

Khuong A, Gautrais J, Perna A, Sbaï C, Combe M, et al. 2016. Stigmergic construction and topochemical information shape ant nest architecture. *Proc Natl Acad Sci U S A*. 113(5):1303–8

Kim HY, Davidson LA. 2011. Punctuated actin contractions during convergent extension and their permissive regulation by the non-canonical Wnt-signaling pathway. *J Cell Sci*. 124(4):635–46

Koch AJ, Meinhardt H. 1994. Biological pattern formation: from basic mechanisms to complex structures. *Rev Mod Phys*. 66(4):1481–1507

Koenigsberger M, Seppey D, Bény J-L, Meister J-J. 2010. Mechanisms of propagation of intercellular calcium waves in arterial smooth muscle cells. *Biophys J*. 99(2):333–43

Kondo S, Miura T. 2010. Reaction-diffusion model as a framework for understanding biological pattern formation. *Science*. 329(5999):1616–20

Konopka RJ, Benzer S. 1971. Clock mutants of *Drosophila melanogaster*. *Proc Natl Acad Sci U S A*. 68(9):2112–16

Koride S, He L, Xiong L-P, Lan G, Montell DJ, Sun SX. 2014. Mechanochemical regulation of oscillatory follicle cell dynamics in the developing Drosophila egg chamber. *Mol Biol Cell*. 25(22):3709–16

Kovács M, Thirumurugan K, Knight PJ, Sellers JR. 2007. Load-dependent mechanism of nonmuscle myosin 2. *Proc Natl Acad Sci U S A*. 104(24):9994–99

Kryuchkov M, Bilousov O, Lehmann J, Fiebig M, Katanaev VL. 2020. Reverse and forward engineering of Drosophila corneal nanocoatings. *Nature*. 585(7825):383–89

Kumar KV, Bois JS, Jülicher F, Grill SW. 2014. Pulsatory patterns in active fluids. *Phys Rev*

Lett. 112(20):208101

Lecuit T, Lenne P-F, Munro E. 2011. Force generation, transmission, and integration during cell and tissue morphogenesis. *Annu Rev Cell Dev Biol*. 27(1):157–84

Li W, Llopis J, Whitney M, Zlokarnik G, Tsien RY. 1998. Cell-permeant caged InsP3 ester shows that Ca2+ spike frequency can optimize gene expression. *Nature*. 392(6679):936–41

Liu C, Fu X, Liu L, Ren X, Chau CKL, et al. 2011. Sequential establishment of stripe patterns in an expanding cell population. *Science*. 334(6053):238–41

Loose M, Fischer-Friedrich E, Ries J, Kruse K, Schwille P. 2008. Spatial regulators for bacterial cell division self-organize into surface waves in vitro. *Science*. 320(5877):789–92

Lotka AJ. 1920. Undamped oscillations derived from the law of mass action. *J. Am. Chem. Soc.* 42(8):1595–99

Lubensky DK, Pennington MW, Shraiman BI, Baker NE. 2011. A dynamical model of ommatidial crystal formation. *Proc Natl Acad Sci U S A*. 108(27):11145–50

Machacek M, Hodgson L, Welch C, Elliott H, Pertz O, et al. 2009. Coordination of Rho GTPase activities during cell protrusion. *Nature*. 461(7260):99–103

Machado PF, Blanchard GB, Duque J, Gorfinkiel N. 2014. Cytoskeletal turnover and Myosin contractility drive cell autonomous oscillations in a model of Drosophila Dorsal Closure. *Eur Phys J Spec Top*. 223(7):1391–1402

Mahalwar P, Walderich B, Singh AP, Nüsslein-Volhard C. 2014. Local reorganization of xanthophores fine-tunes and colors the striped pattern of zebrafish. *Science*. 345(6202):1362–64

Maini PK. 2004. Using mathematical models to help understand biological pattern formation. *C R Biol*. 327(3):225–34

Maini PK, Woolley TE, Baker RE, Gaffney EA, Lee SS. 2012. Turing's model for biological pattern formation and the robustness problem. *Interface Focus*. 2(4):487–96

Maître J-L, Niwayama R, Turlier H, Nédélec F, Hiiragi T. 2015. Pulsatile cell-autonomous contractility drives compaction in the mouse embryo. *Nat Cell Biol*. 17(7):849–55

Mammoto T, Ingber DE. 2010. Mechanical control of tissue and organ development. *Development*. 137(9):1407–20

Martin AC, Kaschube M, Wieschaus EF. 2009. Pulsed contractions of an actin–myosin network drive apical constriction. *Nature*. 457(7228):495–99

Mayer M, Depken M, Bois JS, Jülicher F, Grill SW. 2010. Anisotropies in cortical tension reveal the physical basis of polarizing cortical flows. *Nature*. 467(7315):617–21

Menshykau D, Michos O, Lang C, Conrad L, McMahon AP, Iber D. 2019. Image-based modeling of kidney branching morphogenesis reveals GDNF-RET based Turing-type mechanism and pattern-modulating WNT11 feedback. *Nat Commun*. 10(1):1–13

Mercker M, Brinkmann F, Marciniak-Czochra A, Richter T. 2016. Beyond Turing: mechanochemical pattern formation in biological tissues. *Biol Direct*. 11(1):22

Mercker M, Köthe A, Marciniak-Czochra A. 2015. Mechanochemical Symmetry Breaking in Hydra Aggregates. *Biophys J*. 108(9):2396–2407

Miao H, Blankenship JT. 2020. The pulse of morphogenesis: actomyosin dynamics and regulation in epithelia. *Development*. 147(17):dev186502

Michaux JB, Robin FB, McFadden WM, Munro EM. 2018. Excitable RhoA dynamics drive pulsed contractions in the early C. elegans embryo. *J Cell Biol*. 217(12):4230–52

Michel M, Dahmann C. 2020. Tissue mechanical properties modulate cell extrusion in the Drosophila abdominal epidermis. *Development*. 147(5):dev179606

Morse ES. 1916. Fireflies flashing in unison. *Science*. 43(1101):169–70

Müller P, Rogers KW, Jordan BM, Lee JS, Robson D, et al. 2012. Differential diffusivity of

Nodal and Lefty underlies a reaction-diffusion patterning system. *Science*. 336(6082):721–24

Munjal A, Philippe J-M, Munro E, Lecuit T. 2015. A self-organized biomechanical network drives shape changes during tissue morphogenesis. *Nature*. 524(7565):351–55

Munro E, Nance J, Priess JR. 2004. Cortical flows powered by asymmetrical contraction transport PAR proteins to establish and maintain anterior-posterior polarity in the early C. elegans embryo. *Dev Cell*. 7(3):413–24

Murray JD, Oster GF. 1984. Generation of biological pattern and form. *Math Med Biol*. 1(1):51–75

Murray JD, Oster GF, Harris AK. 1983. A mechanical model for mesenchymal morphogenesis. *J Math Biol*. 17(1):125–29

Nakamasu A, Takahashi G, Kanbe A, Kondo S. 2009. Interactions between zebrafish pigment cells responsible for the generation of Turing patterns. *Proc Natl Acad Sci U S A*. 106(21):8429–34

Newman SA, Frisch HL. 1979. Dynamics of skeletal pattern formation in developing chick limb. *Science*. 205(4407):662–68

Nishikawa M, Naganathan SR, Jülicher F, Grill SW. 2017. Controlling contractile instabilities in the actomyosin cortex. *eLife*. 6:e19595

Nishimura M, Inoue Y, Hayashi S. 2007. A wave of EGFR signaling determines cell alignment and intercalation in the Drosophila tracheal placode. *Development*. 134(23):4273–82

Novák B, Tyson JJ. 2008. Design principles of biochemical oscillators. *Nat Rev Mol Cell Biol*. 9(12):981–91

Ogura Y, Wen F-L, Sami MM, Shibata T, Hayashi S. 2018. A switch-like activation relay of EGFR-ERK signaling regulates a wave of cellular contractility for epithelial

invagination. *Dev Cell*. 46(2):162-172.e5

Oster GF, Murray JD. 1989. Pattern formation models and developmental constraints. *J Exp Zool*. 251(2):186–202

Owen JP, Yates CA, Kelsh RN. 2021. Differential growth is a critical determinant of zebrafish pigment pattern formation. *bioRxiv*. doi: 10.1101/2021.06.11.448058

Özkaya N, Leger D, Goldsheyder D, Nordin M. 2017. Mechanical properties of biological tissues. In *Fundamentals of Biomechanics: Equilibrium, Motion, and Deformation*, pp. 361–87. Cham: Springer International Publishing

Palmeirim I, Henrique D, Ish-Horowicz D, Pourquié O. 1997. Avian *hairy* gene expression identifies a molecular clock linked to vertebrate segmentation and somitogenesis. *Cell*. 91(5):639–48

Pálsson E, Cox EC. 1996. Origin and evolution of circular waves and spirals in Dictyostelium discoideum territories. *Proc Natl Acad Sci U S A*. 93(3):1151–55

Park H-O, Bi E. 2007. Central roles of small GTPases in the development of cell polarity in yeast and beyond. *Microbiol Mol Biol Rev*. 71(1):48–96

Peleg B, Disanza A, Scita G, Gov N. 2011. Propagating cell-membrane waves driven by curved activators of actin polymerization. *PLOS ONE*. 6(4):e18635

Perna A, Theraulaz G. 2017. When social behaviour is moulded in clay: on growth and form of social insect nests. *J Exp Biol*. 220(1):83–91

Pourquié O. 2003. The segmentation clock: Converting embryonic time into spatial pattern. *Science*. 301(5631):328–30

Purvis JE, Lahav G. 2013. Encoding and decoding cellular information through signaling dynamics. *Cell*. 152(5):945–56

Pye K, Chance B. 1966. Sustained sinusoidal oscillations of reduced pyridine nucleotide in a cell-free extract of Saccharomyces carlsbergensis. *Proc Natl Acad Sci U S A*.

55(4):888–94

Rashevsky N. 1940. An approach to the mathematical biophysics of biological self-regulation and of cell polarity. *Bull Math Biophys*. 2(1):15–25

Raskin DM, Boer PAJ de. 1999. Rapid pole-to-pole oscillation of a protein required for directing division to the middle of Escherichia coli. *Proc Natl Acad Sci U S A*. 96(9):4971–76

Raspopovic J, Marcon L, Russo L, Sharpe J. 2014. Modeling digits. Digit patterning is controlled by a Bmp-Sox9-Wnt Turing network modulated by morphogen gradients. *Science*. 345(6196):566–70

Rauzi M, Lenne P-F, Lecuit T. 2010. Planar polarized actomyosin contractile flows control epithelial junction remodelling. *Nature*. 468(7327):1110–14

Razzell W, Wood W, Martin P. 2014. Recapitulation of morphogenetic cell shape changes enables wound re-epithelialisation. *Development*. 141(9):1814–20

Ready DF, Chang HC. 2021. Calcium waves facilitate and coordinate the contraction of endfeet actin stress fibers in Drosophila interommatidial cells. *bioRxiv*. doi: 10.1101/2021.04.08.439074

Ready DF, Hanson TE, Benzer S. 1976. Development of the Drosophila retina, a neurocrystalline lattice. *Dev Biol*. 53(2):217–40

Reddy P, Zehring WA, Wheeler DA, Pirrotta V, Hadfield C, et al. 1984. Molecular analysis of the period locus in Drosophila melanogaster and identification of a transcript involved in biological rhythms. *Cell*. 38(3):701–10

Ren Y, Effler JC, Norstrom M, Luo T, Firtel RA, et al. 2009. Mechanosensing through cooperative interactions between myosin II and the actin crosslinker cortexillin I. *Curr Biol*. 19(17):1421–28

Rodríguez-Franco P, Brugués A, Marín-Llauradó A, Conte V, Solanas G, et al. 2017. Long-

lived force patterns and deformation waves at repulsive epithelial boundaries. *Nat Mater*. 16(10):1029–37

Rogers KW, Lord ND, Gagnon JA, Pauli A, Zimmerman S, et al. 2017. Nodal patterning without Lefty inhibitory feedback is functional but fragile. *eLife*. 6:e28785

Roth S, Lynch JA. 2009. Symmetry breaking during Drosophila oogenesis. *Cold Spring Harb Perspect Biol*. 1(2):a001891

Ryan GL, Petroccia HM, Watanabe N, Vavylonis D. 2012a. Excitable actin dynamics in lamellipodial protrusion and retraction. *Biophys J*. 102(7):1493–1502

Ryan GL, Watanabe N, Vavylonis D. 2012b. A review of models of fluctuating protrusion and retraction patterns at the leading edge of motile cells. *Cytoskeleton*. 69(4):195–206

Sarfati R, Hayes JC, Peleg O. 2021. Self-organization in natural swarms of Photinus carolinus synchronous fireflies. *Sci Adv*. 7(28):eabg9259

Schauer A, Pinheiro D, Hauschild R, Heisenberg C-P. 2020. Zebrafish embryonic explants undergo genetically encoded self-assembly. *eLife*. 9:e55190

Scholes NS, Schnoerr D, Isalan M, Stumpf MPH. 2019. A comprehensive network atlas reveals that Turing patterns are common but not robust. *Cell Syst*. 9(3):243-257.e4

Schweisguth F, Corson F. 2019. Self-Organization in Pattern Formation. *Developmental Cell*. 49(5):659–77

Scoones JC, Hiscock TW. 2020. A dot-stripe Turing model of joint patterning in the tetrapod limb. *Development*. 147(8):dev183699

Segel LA, Jackson JL. 1972. Dissipative structure: An explanation and an ecological example. *J Theor Biol*. 37(3):545–59

Sekine R, Shibata T, Ebisuya M. 2018. Synthetic mammalian pattern formation driven by differential diffusivity of Nodal and Lefty. *Nat Commun*. 9(1):1–11

Serra-Picamal X, Conte V, Vincent R, Anon E, Tambe DT, et al. 2012. Mechanical waves during tissue expansion. *Nat Phys*. 8(8):628–34

Shlomovitz R, Gov NS. 2007. Membrane waves driven by actin and myosin. *Phys Rev Lett*. 98(16):168103

Shyer AE, Rodrigues AR, Schroeder GG, Kassianidou E, Kumar S, Harland RM. 2017. Emergent cellular self-organization and mechanosensation initiate follicle pattern in the avian skin. *Science*. 357(6353):811–15

Simões S, Oh Y, Wang MFZ, Fernandez-Gonzalez R, Tepass U. 2017. Myosin II promotes the anisotropic loss of the apical domain during Drosophila neuroblast ingression. *J Cell Biol*. 216(5):1387–1404

Simunovic M, Metzger JJ, Etoc F, Yoney A, Ruzo A, et al. 2019. A 3D model of a human epiblast reveals BMP4-driven symmetry breaking. *Nat Cell Biol*. 21(7):900–910

Slaughter BD, Smith SE, Li R. 2009. Symmetry Breaking in the Life Cycle of the Budding Yeast. *Cold Spring Harb Perspect Biol*. 1(3):a003384

Solon J, Kaya-Çopur A, Colombelli J, Brunner D. 2009. Pulsed forces timed by a ratchet-like mechanism drive directed tissue movement during dorsal closure. *Cell*. 137(7):1331–42

Staddon MF, Munro EM, Banerjee S. 2021. Pulsatile contractions and pattern formation in excitable active gels. *bioRxiv*. doi: 10.1101/2021.02.22.432369

Theraulaz G, Bonabeau E, Nicolis SC, Solé RV, Fourcassié V, et al. 2002. Spatial patterns in ant colonies. *Proc Natl Acad Sci U S A*. 99(15):9645–49

Thomas D. 1976. Artificial enzyme membranes. Transport, memory and oscillatory phenomena. In *Analysis and Control of Immobilized Enzyme Systems : Proceedings of an International Symposium*, pp. 115–50. Amsterdam: North-Holland ; New York : American Elsevier

Tkachenko E, Sabouri-Ghomi M, Pertz O, Kim C, Gutierrez E, et al. 2011. Protein Kinase A governs a RhoA-RhoGDI protrusion-retraction pacemaker in migrating cells. *Nat Cell Biol*. 13(6):660–67

Tlili S, Gauquelin E, Li B, Cardoso O, Ladoux B, et al. 2018. Collective cell migration without proliferation: density determines cell velocity and wave velocity. *R Soc Open Sci*. 5(5):172421

Tsai TY-C, Choi YS, Ma W, Pomerening JR, Tang C, James E. Ferrell J. 2008. Robust, Tunable Biological Oscillations from Interlinked Positive and Negative Feedback Loops. *Science*

Turing AM. 1952. The chemical basis of morphogenesis. *Philos Trans R Soc Lond B Biol Sci*. 237(641):37–72

Veerman F, Mercker M, Marciniak-Czochra A. 2021. Beyond Turing: Far-from-equilibrium patterns and mechano-chemical feedback. *bioRxiv*. doi:10.1101/2021.03.10.434636

Vergassola M, Deneke VE, Talia SD. 2018. Mitotic waves in the early embryogenesis of Drosophila: Bistability traded for speed. *Proc Natl Acad Sci U S A*. 115(10):E2165–74

Vicker MG. 2002. F-actin assembly in Dictyostelium cell locomotion and shape oscillations propagates as a self-organized reaction–diffusion wave. *FEBS Letters*. 510(1–2):5–9

Volterra V. 1926. Fluctuations in the abundance of a species considered mathematically. *Nature*. 118(2972):558–60

Wagner EL, Shin J-B. 2019. Mechanisms of Hair Cell Damage and Repair. *Trends in Neurosciences*. 42(6):414–24

Walton KD, Mishkind D, Riddle MR, Tabin CJ, Gumucio DL. 2018. Blueprint for an intestinal villus: Species-specific assembly required. *Wiley Interdiscip Rev Dev Biol*. 7(4):e317

Warmflash A, Sorre B, Etoc F, Siggia ED, Brivanlou AH. 2014. A method to recapitulate early embryonic spatial patterning in human embryonic stem cells. *Nat Methods*. 11(8):847–54

Watanabe M, Kondo S. 2015a. Fish pigmentation. Comment on "Local reorganization of xanthophores fine-tunes and colors the striped pattern of zebrafish." *Science*. 348(6232):297

Watanabe M, Kondo S. 2015b. Is pigment patterning in fish skin determined by the Turing mechanism? *Trends Genet*. 31(2):88–96

Wedlich-Soldner R, Altschuler S, Wu L, Li R. 2003. Spontaneous cell polarization through actomyosin-based delivery of the Cdc42 GTPase. *Science*. 299(5610):1231–35

Wedlich-Söldner R, Betz T. 2018. Self-organization: the fundament of cell biology. *Philosophical Transactions of the Royal Society B: Biological Sciences*. 373(1747):20170103

Weiner OD, Marganski WA, Wu LF, Altschuler SJ, Kirschner MW. 2007. An actin-based wave generator organizes cell motility. *PLOS Biol*. 5(9):e221

Wettmann L, Kruse K. 2018. The Min-protein oscillations in Escherichia coli: an example of self-organized cellular protein waves. *Philos Trans R Soc Lond B Biol Sci*. 373(1747):20170111

Wigbers MC, Tan TH, Brauns F, Liu J, Swartz SZ, et al. 2021. A hierarchy of protein patterns robustly decodes cell shape information. *Nat Phys*. 17(5):578–84

Yang Y, Wu M. 2018. Rhythmicity and waves in the cortex of single cells. *Philos Trans R Soc Lond B Biol Sci*. 373(1747):20170116

Yu JC, Fernandez-Gonzalez R. 2016. Local mechanical forces promote polarized junctional assembly and axis elongation in Drosophila. *eLife*. 5:e10757

Zehring WA, Wheeler DA, Reddy P, Konopka RJ, Kyriacou CP, et al. 1984. P-element

transformation with period locus DNA restores rhythmicity to mutant, arrhythmic drosophila melanogaster. *Cell*. 39(2, Part 1):369–76

Zhang S, Teng X, Toyama Y, Saunders TE. 2020. Periodic oscillations of myosin-II mechanically proofread cell-cell connections to ensure robust formation of the cardiac vessel. *Curr Biol*. 30(17):3364-3377.e4

FIGURE CAPTIONS

Figure 1. Chemical Turing patterns:

(**A**) Generation of a pattern with finite wavelength from random fluctuations. (**B**) (**Top**) Schemas of the most simple reaction motifs needed to form a Turing pattern using an activator-inhibitor or substrate depletion system. (**Bottom**) Schematic view of the concentration profiles that result from the interactions shown above. Figure adapted from (Halatek et al. 2018). (**C**) Simulated Turing patterns that result from linear reaction-diffusion equations, where red is the activator concentration. Only the strength with which the inhibitor acts the activator is varied. Figure generated using the Turing simulator described in (Kondo & Miura 2010). (**D**) (**left**) Evolution of GFP-Cdc42 distribution in a budding yeast. Figure adapted with (pending) permission from (Slaughter et al. 2009). (**right**) Simplified model of the substrate depletion that leads to the polarization. (**E**) (**left**) Picture of a mouse palate and in situ hybridization for Shh in wildtype mice and mice with FGF (SU5402) or Hedgehog (cyclopamine) inhibitors. Figure adapted with (pending) permission from (Economou et al. 2012). (**right**) Simplified model showing how the interactions between FGF and Shh lead to patterned rugae formation. (**F**) An initially uniform distribution of dead ants is rearranged by worker ants to form piles following a simple Turing mechanism. Figure adapted from (Theraulaz et al. 2002); copyright 2002 National Academy of Sciences.

Figure 2. Temporal chemical patterns.

(**A**) Oscillatory system. (**left**) A, activator, I, inhibitor. k_A, k_I are the reaction rates. (**middle**) Concentration evolution of the activator [A] and of the inhibitor [I], with the same period but a phase shift. (**right**) Phase plot showing a limit cycle. (**B**) Excitable system. (**left**) A positive feedback is now present. (**middle**) Concentration evolution of the activator [A]. (**right**) Phase plot with a limit cycle. The S-shape continuous line is the A-nullcline, i.e. the line with $\partial[A]/\partial t=0$. The straight line is the I-nullcline. In red is the basin of attraction of the upper branch of the cycle, in blue the one from the lower branch. The dashed line shows the threshold values between both (eg. above which A dominates). Figure adapted from (Gelens et al. 2014). (**C-E**) Migration in *Dictyostelium*. (**C**) Experimental TIRF data at cell edge and quantification showing fast oscillations of F-actin regulators. Blue, Coronin-GFP. Red, LimE-RFP (F-actin sensor). (**D**) Data-driven network and proposed computer model with slow (STEN) and fast (CON) oscillators. Arp2/3 – F-actin – Coronin make the activator/inhibitor module, abstracted as X_f and Y_f in the simulation. Dashed arrows: indirect or hypothetical interaction. (**E**) Time evolution of oscillator networks (**left**) and the cellular processes they control (high frequency undulations and low frequency protrusions). Figure C,D,E adapted with (pending) permission from (Huang et al. 2013).

Figure 3. Chemical trigger waves.

(**A**) Propagation of a wave in a bistable system. Spatial diagram (**left**) and phase plot (**right**). Increased concentration of the activator by diffusion (light red) from the high activator zone and reaction (dark red) allows the threshold to be crossed and a wave to propagate. Figure adapted from (Gelens et al. 2014). (**B**) Surface contraction waves in a starfish oocyte overexpressing Ect2.The image shows the difference in signal at two different time points from a Rho-GTP sensor (GFP-rGBD). The white rectangle shows where the kymograph is drawn

(**middle**). The Cdk1 gradient is produced by the asymmetrically positioned nucleus. Its decay leads to the activation of the activator/inhibitor module constituted by Rho-GTP and F-actin. Figure adapted with (pending) permission from (Bement et al. 2015). (**C**) Mitotic waves in the *Drosophila* embryo depend on Cdk1 waves. (**left**) Red dots are histone-RFP. Figure adapted with (pending) permission from (Deneke et al. 2016).

Figure 4. Mechanical Turing-like patterns

(**A**) Motor-dependent contractility induces cytoskeletal flow, which advects more motors and causes the accumulation of more contractile elements (positive feedback). It therefore acts like an activator. The induced flow causes friction which counteracts flow and thereby contraction. Friction therefore acts as an inhibitor. (**B**) Cell contractility leads to buildup in stress in the extracellular matrix and the accumulation of more contractile elements. It therefore acts like an activator. The buildup of elastic stress prevents further deformation of the matrix which in turn counteracts contraction. It therefore acts as an inhibitor. (**C**) Images of *Drosophila* tracheal tubules where the friction is decreased or removed, thereby changing the pattern of actin rings. Figure adapted from (Hannezo et al. 2015). (**D**) Development of clusters of fibroblasts from an initially random distribution. Figure adapted from (Harris et al. 1984). (**E**) Images of avian skin where the pattern of feather follicle primordia changes with changing substrate stiffness. Figure adapted with (pending) permission from (Shyer et al. 2017). (**F**) (**top**) Polarized formation of a pseudopod during neutrophil migration. Figure adapted with (pending) permission from (Houk et al. 2012). (**bottom**) A schema showing the interactions between molecular components and tensile forces that underlies cell polarization. (**G**) (**top**) An image of localized Gdf1 expression in a quail embryo and a snapshot of cell trajectories. Figure adapted with (pending) permission from (Caldarelli et al. 2021). (**bottom**) A schema showing the interactions that drive the pattern formation.

Figure 5. Mechanochemical spatial-temporal patterns.

(**A**) Actomyosin pulse. (**top**) Experimental data and quantification of a Rho-GTP (aniRBD-GFP) and MyoII (MRLC-mCherry) pulse. (**bottom**) Amplification mechanism. Green fibers are actin fibers, orange are MyoII motors, blue arrows are advection. The negative feedback terminating the pulse is hypothetical (dashed arrow). Figure adapted from (Munjal et al. 2015). (**B**) ERK waves in cell culture. (**left**) Experimental data and quantification (kymograph) of ERK activity (FRET/CFP ratio from EKAREV-NLS) in the migrating epithelium. (**right**) Model proposed, with contraction as a short-range inhibitor/long range activator. Figure adapted with (pending) permission from (Hino et al. 2020). (**C,D**) *Drosophila* presumptive midgut invagination wave. (**C**) Experimental data of MyoII (MRLC) in the epithelium. A line of cells is highlighted in yellow, another in white. (**D**) (**left**) Model proposed, with invagination as a short-range inhibitor/long range activator of adhesion and contractility. (**right**) Transversal view of the epithelium showing the mechanical cycle. Figure adapted from (Bailles et al. 2019).

Figure 1

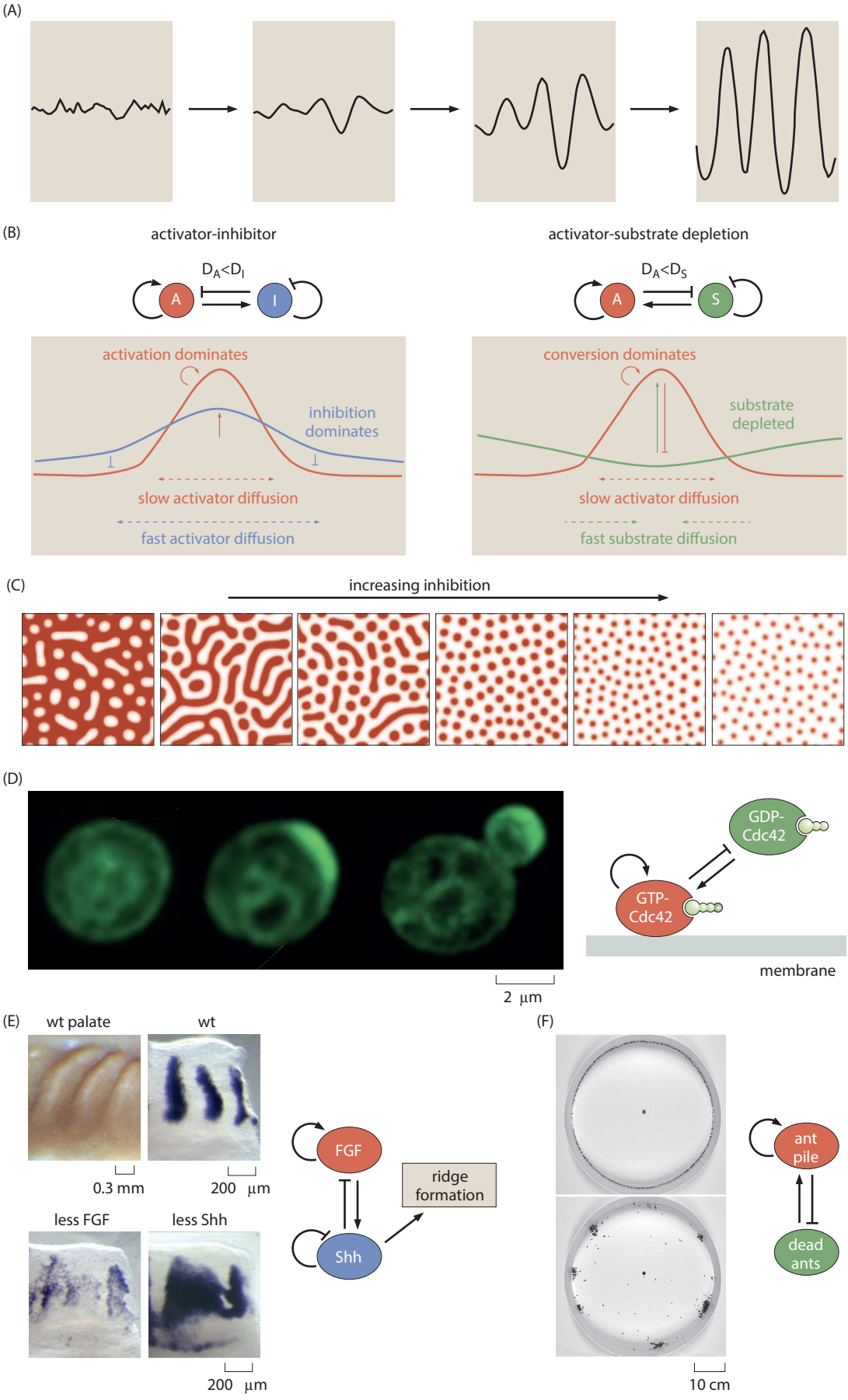
(A)
(B)
activator-inhibitor
activator-substrate depletion
$D_A<D_I$
A
I
$D_A<D_S$
A
S
activation dominates
inhibition dominates
slow activator diffusion
fast activator diffusion
conversion dominates
substrate depleted
slow activator diffusion
fast substrate diffusion
(C)
increasing inhibition
(D)
2 µm
GDP-Cdc42
GTP-Cdc42
membrane
(E)
wt palate
wt
0.3 mm
200 µm
less FGF
less Shh
200 µm
FGF
Shh
ridge formation
(F)
ant pile
dead ants
10 cm

Figure 2

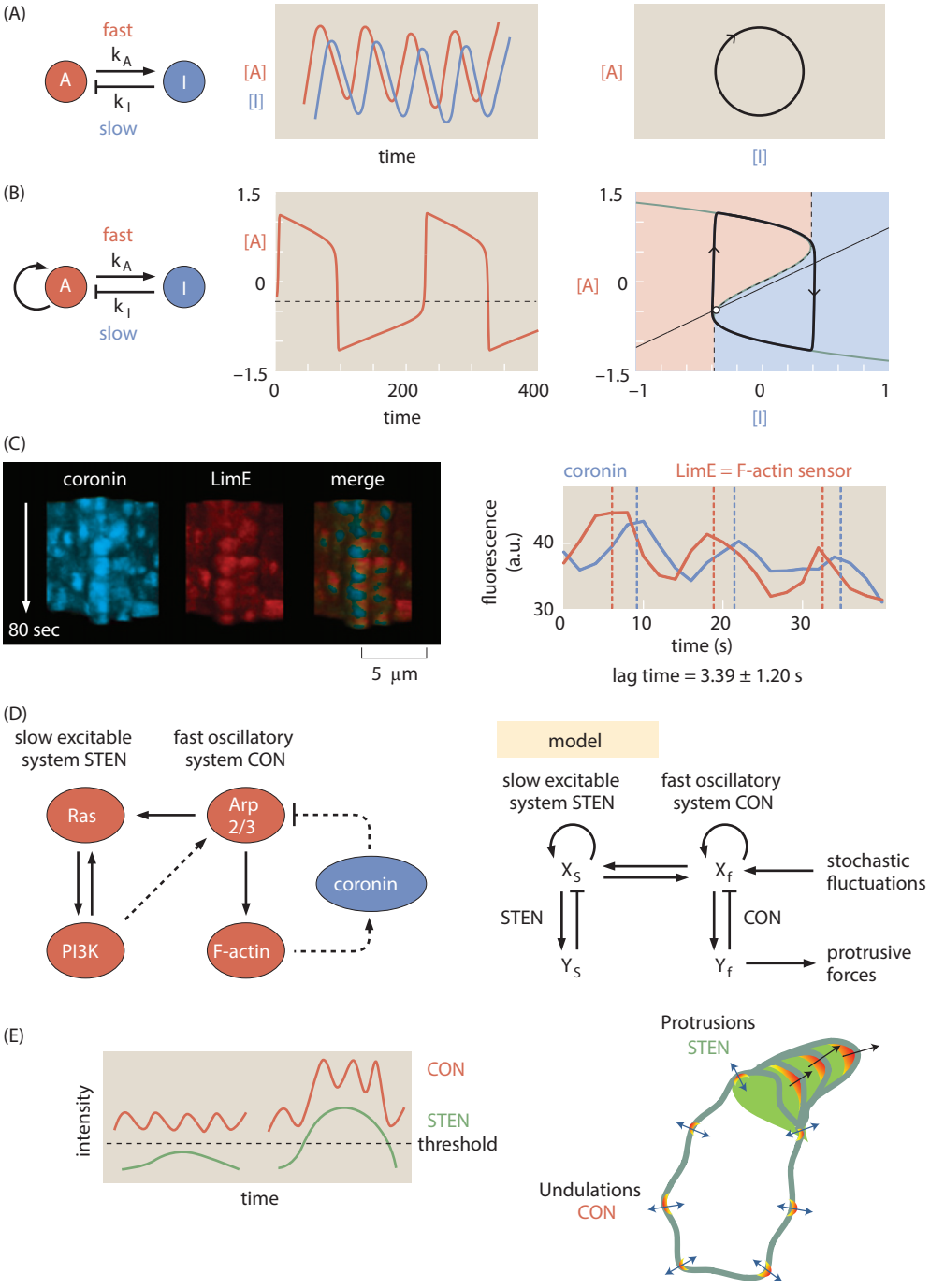
(A)
fast
k_A
A
I
k_I
slow
[A]
[I]
time
[A]
[I]
(B)
fast
k_A
A
I
k_I
slow
1.5
[A]
0
−1.5
0
200
400
time
1.5
[A]
0
−1.5
−1
0
1
[I]
(C)
coronin
LimE
merge
80 sec
5 µm
coronin
LimE = F-actin sensor
fluorescence (a.u.)
40
30
0
10
20
30
time (s)
lag time = 3.39 ± 1.20 s
(D)
slow excitable system STEN
fast oscillatory system CON
Ras
Arp 2/3
coronin
PI3K
F-actin
model
slow excitable system STEN
fast oscillatory system CON
X_S
X_f
stochastic fluctuations
STEN
CON
Y_S
Y_f
protrusive forces
(E)
intensity
CON
STEN
threshold
time
Protrusions
STEN
Undulations
CON

Figure 3

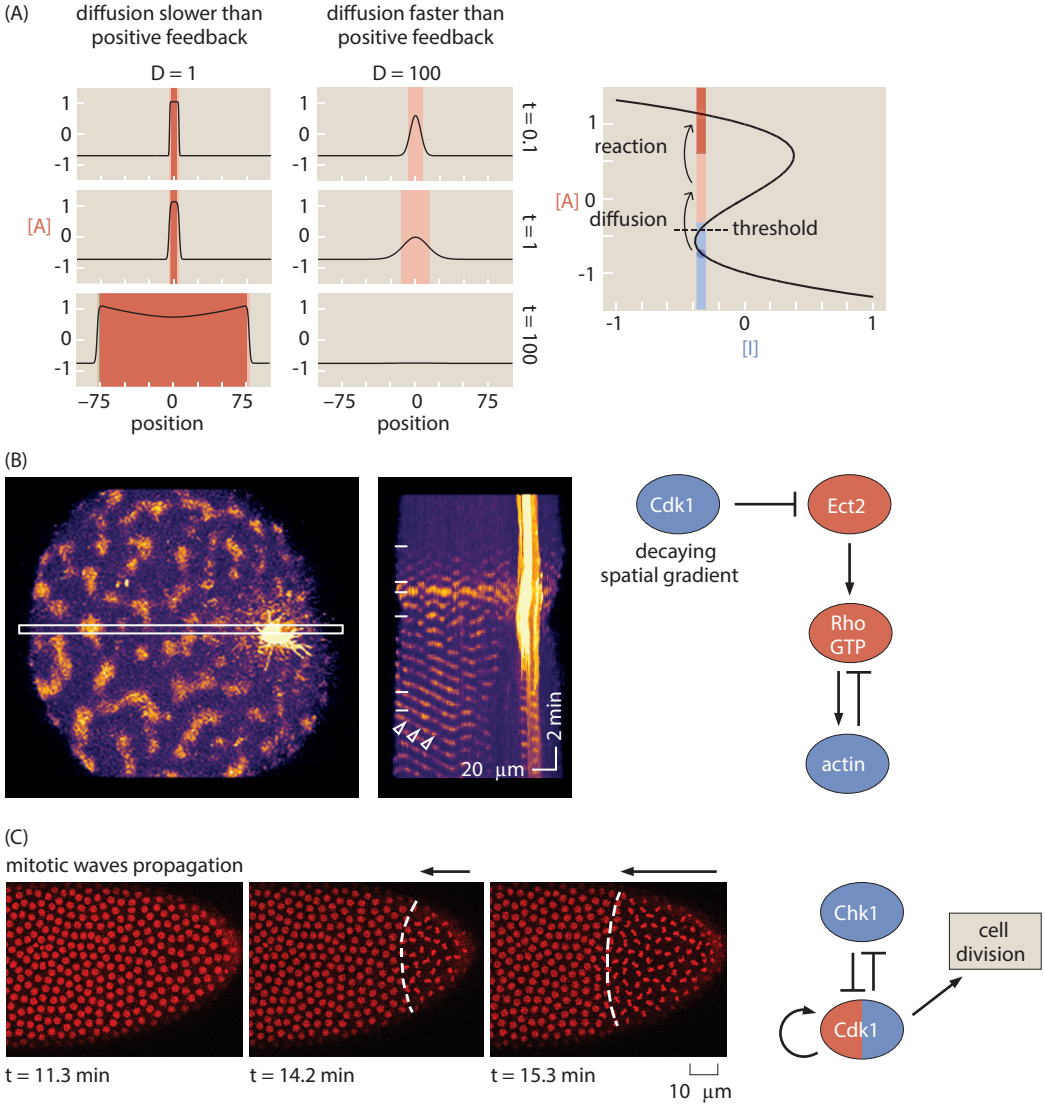
(A)
diffusion slower than positive feedback
diffusion faster than positive feedback
D = 1
D = 100
t = 0.1
t = 1
t = 100
[A]
position
reaction
diffusion
threshold
[I]
(B)
2 min
20 µm
Cdk1
Ect2
decaying spatial gradient
Rho GTP
actin
(C)
mitotic waves propagation
t = 11.3 min
t = 14.2 min
t = 15.3 min
10 µm
Chk1
Cdk1
cell division

Figure 4

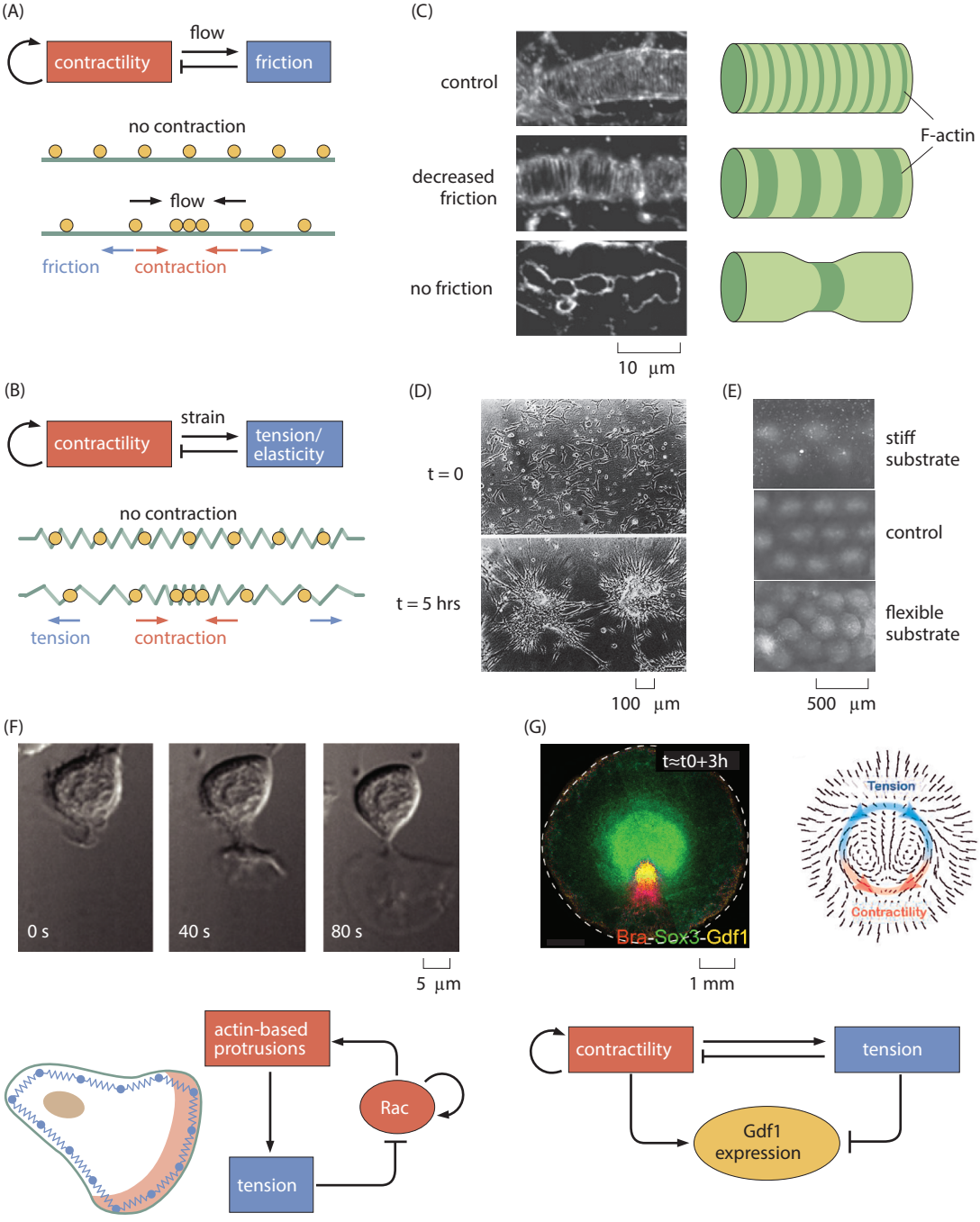
(A)
contractility
flow
friction
no contraction
flow
friction
contraction
(B)
contractility
strain
tension/
elasticity
no contraction
tension
contraction
(C)
control
decreased
friction
no friction
F-actin
10 µm
(D)
t = 0
t = 5 hrs
100 µm
(E)
stiff
substrate
control
flexible
substrate
500 µm
(F)
0 s
40 s
80 s
5 µm
(G)
t≈t0+3h
Bra-Sox3-Gdf1
1 mm
Tension
Contractility
actin-based
protrusions
Rac
tension
contractility
tension
Gdf1
expression

Figure 5

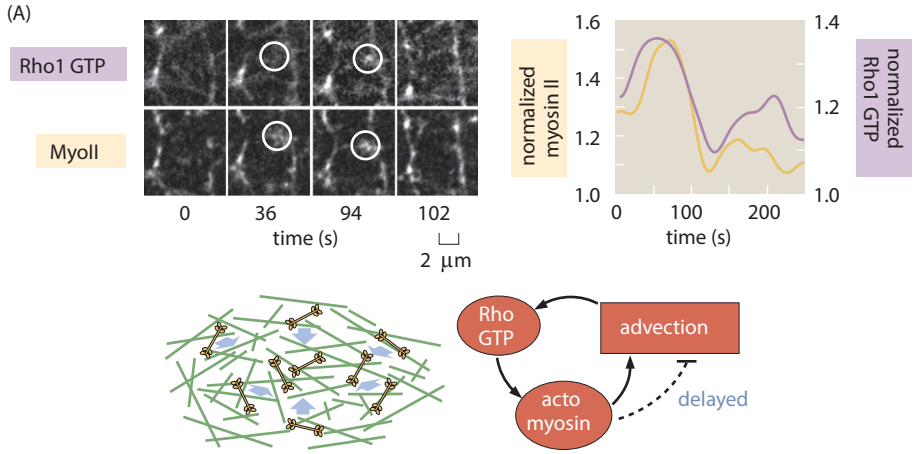
(A)
Rho1 GTP
MyoII
0
36
94
102
time (s)
2 µm
normalized myosin II
normalized Rho1 GTP
1.6
1.4
1.2
1.0
0
100
200
time (s)
Rho GTP
advection
acto myosin
delayed

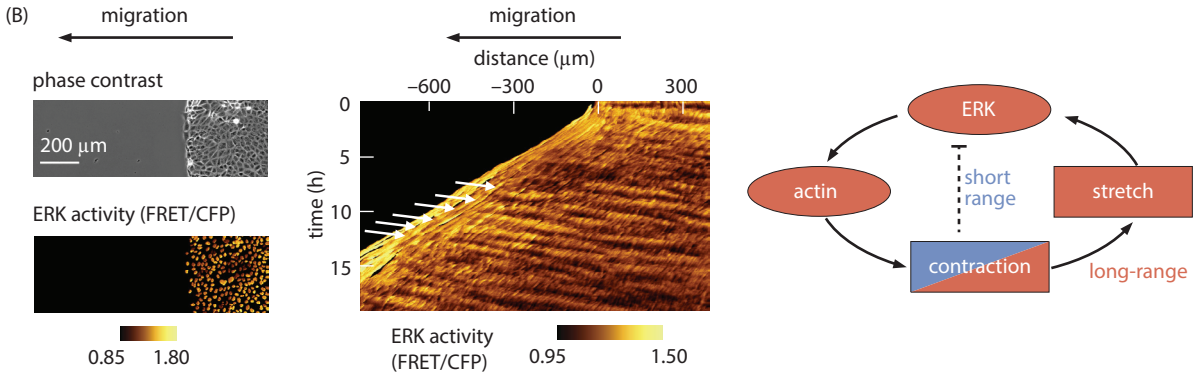
(B)
migration
phase contrast
200 µm
ERK activity (FRET/CFP)
0.85
1.80
migration
distance (µm)
−600
−300
0
300
time (h)
0
5
10
15
ERK activity (FRET/CFP)
0.95
1.50
ERK
actin
short range
stretch
contraction
long-range

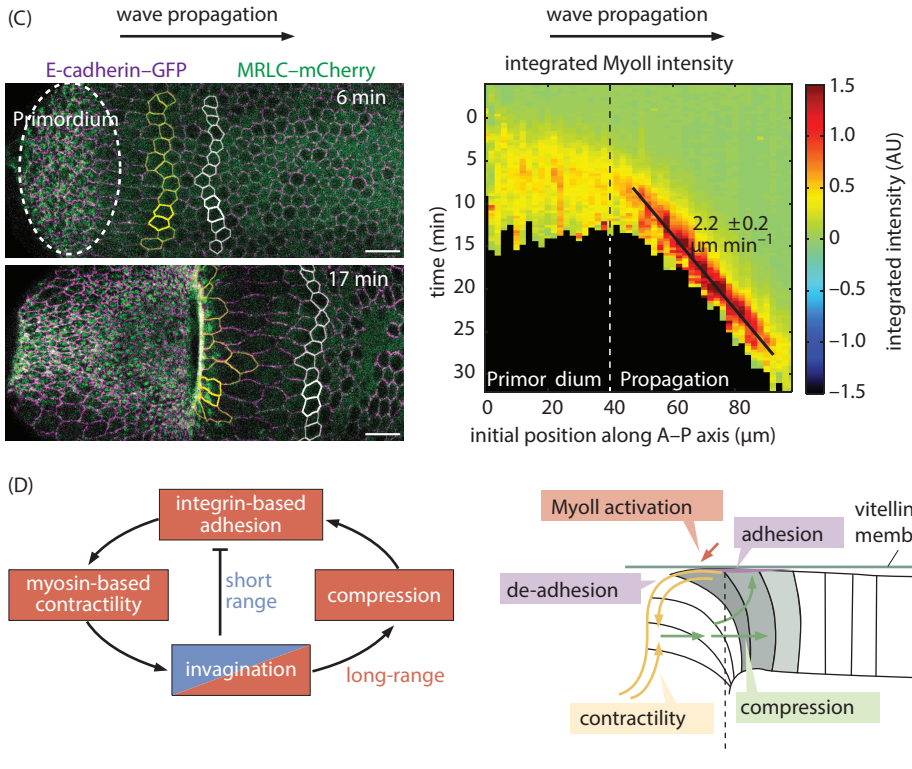
(C)
wave propagation
E-cadherin–GFP
MRLC–mCherry
Primordium
6 min
17 min
wave propagation
integrated MyoII intensity
time (min)
0
5
10
15
20
25
30
2.2 ±0.2 µm min−1
Primor dium
Propagation
0
20
40
60
80
initial position along A–P axis (µm)
1.5
1.0
0.5
0
−0.5
−1.0
−1.5
integrated intensity (AU)

(D)
integrin-based adhesion
myosin-based contractility
short range
compression
invagination
long-range
MyoII activation
adhesion
vitelline membrane
de-adhesion
contractility
compression